HELSINGIN YLIOPISTO — HELSINGFORS UNIVERSITET — UNIVERSITY OF HELSINKI

Tiedekunta/Osasto — Fakultet/Sektion — Faculty	Laitos — Institution — Department
Faculty of Science	Department of Mathematics and Statistics

Tekijä — Författare — Author
Brittany Rose

Työn nimi — Arbetets titel — Title

Evolution of pathogen mutation probabilities

Oppiaine — Läroämne — Subject
Biomathematics

Työn laji — Arbetets art — Level	Aika — Datum — Month and year	Sivumäärä — Sidoantal — Number of pages
Master's Thesis	May 2017	44

Tiivistelmä — Referat — Abstract

Recent biomathematical literature has suggested that, under the assumption of a trade-off between replication speed and fidelity, a pathogen can evolve to more than one optimal mutation rate. O'Fallon (2011) presents a particularly compelling case grounded in simulation. In this thesis, we treat the subject analytically, approaching it through the lens of adaptive dynamics. We formulate a within-host model of the pathogen load starting from assumptions at the genomic level, explicitly accounting for the fact that most mutations are deleterious and stunt growth. We single out the pathogen's mutation probability as the evolving trait that distinguishes strains from one another. Our between-host dynamics take the form of an SI model, first without superinfection and later with two types of non-smooth superinfection function. The pathogen's virulence and transmission rate are functions of the within-host equilibrium pathogen densities. In the case of our mechanistically defined superinfection function, we uncover evolutionary branching in conjunction with two transmission functions, one a caricatural (expansion) example, the other a more biologically realistic (logistic) one. Because of the non-smoothness of the mechanistic superinfection function, our branching points are actually one-sided ESSs à la Boldin & Diekmann (2014). When branching occurs, two strains with different mutation probabilities both ultimately persist on the evolutionary timescale.

Avainsanat — Nyckelord — Keywords
Adaptive dynamics, pathogen, mutation probability, superinfection, critical function analysis

Säilytyspaikka — Förvaringsställe — Where deposited
Kumpula Science Library

Muita tietoja — Övriga uppgifter — Additional information

Evolution of pathogen mutation probabilities

Brittany Rose

MASTER'S THESIS, May 2017

Biomathematics Research Group
Department of Mathematics and Statistics
Faculty of Science
UNIVERSITY OF HELSINKI

Abstract

Recent biomathematical literature has suggested that, under the assumption of a trade-off between replication speed and fidelity, a pathogen can evolve to more than one optimal mutation rate. O'Fallon (2011) presents a particularly compelling case grounded in simulation. In this thesis, we treat the subject analytically, approaching it through the lens of adaptive dynamics. We formulate a within-host model of the pathogen load starting from assumptions at the genomic level, explicitly accounting for the fact that most mutations are deleterious and stunt growth. We single out the pathogen's mutation probability as the evolving trait that distinguishes strains from one another. Our between-host dynamics take the form of an SI model, first without superinfection and later with two types of non-smooth superinfection function. The pathogen's virulence and transmission rate are functions of the within-host equilibrium pathogen densities. In the case of our mechanistically defined superinfection function, we uncover evolutionary branching in conjunction with two transmission functions, one a caricatural (expansion) example, the other a more biologically realistic (logistic) one. Because of the non-smoothness of the mechanistic superinfection function, our branching points are actually one-sided ESSs à la Boldin & Diekmann (2014). When branching occurs, two strains with different mutation probabilities both ultimately persist on the evolutionary timescale.

Acknowledgments

First and foremost, I want to thank Éva Kisdi for her thoughtful guidance and unwavering support during my completion of this master's thesis. Thanks also go to Tadeáš Přiklopil, who helped me get started and shape this project into what it would become. I wish to extend further gratitude to both of them as well as to Stefan Geritz for the excellent teaching that equipped me with the skills necessary to complete this work.

Many thanks are due to my parents, Bob and Alexann, and to my sister, Rebecca, whose love and encouragement anchor my life despite the ocean between us. Finally, I want to thank Tom, Caterina, Juan and Ida for supporting me as I undertook this thesis and for generally filling my days with light.

Contents

1 Introduction

How does a pathogen's mutation rate influence its long-term evolutionary fitness in its host population? This thesis provides a biomathematical framework for addressing this question.

1.1 Motivation

When pathogens copy their genetic material during the replication process, a number of physiological constraints limit their accuracy. Often, an increase in replication fidelity comes at the cost of slower growth. In some cases, such as that of DNA pathogens, this is due in part to the fact that the pathogen must allocate some of its resources to proofreading [12]. Because these resources are finite, investing more of them in replication – thereby increasing the pathogen's intrinsic growth rate – often implies divesting them from proofreading, which allows more mutations to escape undetected.

Although exceptions exist, most RNA viruses lack proofreading mechanisms [7] [16]. These pathogens generally exhibit mutation rates that are orders of magnitude higher than those of their DNA counterparts, despite the fact that deleterious mutations occur far more frequently than beneficial ones [9]. However, there is evidence to suggest that the same trade-off between replication speed and fidelity exists in many RNA viruses, such as HIV-1 and vesicular stomatitis virus (VSV). HIV-1 must devote "energy and/or time [to] base recognition, nucleotide synthesis, and/or polymerase translocation" in order for its polymerase to incorporate the correct base when copying viral RNA (i.e. for replication to be accurate) [6]. Furió et al. showed that "[in VSV] mutants carrying single amino acid substitutions in the RNA polymerase gene, ... changes leading to lower mutation rates also [lead] to slower growth rates" [8] [9].

The trade-off between replication speed and fidelity has been treated mathematically by a number of authors, including [14] and [15]. Using very different modeling techniques, both O'Fallon (2011) and Regoes et al. (2013) find that accounting for this trade-off can reveal two optimal mutation rates for the pathogen. Regoes et al. present a single-infection optimization model in which there are sometimes two candidate optima, but the pathogen ul-

timately evolves to one or the other; there is no coexistence. When two possible optima exist, they occur at the intersection points of a fitness ridge and a biochemical speed-fidelity trade-off function.

In the very work that inspired this thesis, O'Fallon studies the long-term persistence of a pathogen subject to mutations deleterious to its growth rate. He presents a nested model of the within- and between-host dynamics of this pathogen, in which both the disease-induced mortality (virulence) and the transmission rate depend on the pathogen load within the host. He conducts a series of simulations to determine which mutation rates enable the pathogen to persist at high densities through many time steps. Whether parameters are selected to represent acute or chronic infections, pathogens with intermediate replication rates achieve peaks in their long-term population-level prevalence at two distinct mutation rates: one low, the other high.

This result stems in part from the fact that the pathogen's mutation rate influences the duration of the infection. Because of the speed-fidelity trade-off, pathogens that mutate slowly also grow slowly, and they do not achieve high enough within-host prevalence to kill their hosts. Similarly, pathogens that mutate very rapidly acquire too many deleterious mutations to achieve high within-host prevalence, and again their hosts remain alive and infectious for a long time. In both cases, this long infectious period affords the pathogen ample opportunity to infect more hosts, which results in high population-level prevalence of the disease.

Like O'Fallon, we investigate the relationship between a pathogen's mutation rate and its long-term evolutionary fitness, taking into account the trade-off between replication speed and fidelity. However, we take an analytical approach in lieu of a simulative one. We utilize the theory of adaptive dynamics to study competition between pathogen strains with different mutation probabilities, and we seek out evolutionary branching points. These are combinations of strategies (strains) that can coexist in the host population on the evolutionary timescale.

We begin by modeling the dynamics of the pathogen load within the host from assumptions about mutation at the genomic level. Similarly to O'Fallon, we operate on the premise that deleterious mutations stunt the growth of the pathogen. To formulate our between-host dynamics, which take the form of an SI model with superinfection, we follow the work of

Boldin & Diekmann (2008). Our model includes one biological assumption that theirs does not: We suppose that any difference in pathogen strains' growth rates is a direct result of a difference in their mutation rates.

We, like O'Fallon, link our between-host dynamics to the within-host dynamics via transmission and virulence functions that depend on the pathogen density within the host. In the manner of Boldin & Diekmann, we introduce a population-level superinfection function that gives the probability with which an invading pathogen strain replaces the one present in an infected host. We derive two possible definitions (deterministic and mechanistic) for this function, both recovered from the pathogen's host-level behavior. Our mechanistic case diverges from Boldin & Diekmann's.

We perform an adaptive dynamics analysis of the pathogen's between-host dynamics to identify and characterize evolutionary branching points. The following subsection provides an introduction to the methods in adaptive dynamics needed to accomplish this task.

1.2 Methods: adaptive dynamics

Adaptive dynamics is a mathematical theory used to study trait evolution in populations of asexual organisms. Its main concepts and methods, summarized here, are thoroughly detailed in [10].

At the core of adaptive dynamics lie four key assumptions:

1. Individuals reproduce clonally, and mutant offspring are rare.

2. The timescale of selection is much faster than that of mutation. In other words, the population always reaches an attractor before a new mutant arises.

3. When a mutant first appears, it is rare such that its population density is extremely low compared to that of the resident.

4. Phenotypic mutations are random and small (but not infinitesimal).

Consider a population in which all individuals share a strategy (trait) with value x. This could be, for example, the size of a plant's seeds or the virulence of a pathogen. When a mutant (an individual with a different value

for this trait, say y) enters the equilibrated resident population, it will either invade (increase in number) or simply die out.

To determine whether invasion is possible, we calculate the mutant's so-called *invasion fitness*, $s_x(y)$. This is the mutant's long-term exponential growth rate when introduced in small quantity to the resident population. If $s_x(y) < 0$, the mutant is bound for extinction and will not invade. If $s_x(y) > 0$, the mutant has a positive probability of invading. Whether or not it actually does so rests partially on luck: Even a deterministically excellent mutant may be driven to swift extinction by unfortunate stochastic events while it is still relatively rare (strictly speaking, present in finite numbers). Because the resident population is fixed at its steady state value for trait x, the invasion fitness of any neutral mutant ($y = x$) is $s_x(x) = 0$.

To visually assess whether a strategy can be invaded, we turn to the *pairwise invasibility plot* (PIP). This is a plot of the sign of $s_x(y)$ at different combinations of x and y. Two examples appear in figure 1.

Taking the derivative of $s_x(y)$ with respect to y and evaluating the result at $y = x$, we recover the *selection gradient*, $\frac{\partial s_x(y)}{\partial y}\big|_{y=x}$. Setting the selection gradient equal to zero and solving for y, we obtain so-called *singular strategies* x^*. These are fitness maxima and minima, that is, the best (and worst) trait values an individual can take as far as invasion is concerned.

If $\frac{\partial^2 s_x(y)}{\partial y^2}\big|_{y=x=x^*} < 0$, then x^* is a (local) maximum of $s_x(y)$ and is thus an *evolutionarily stable strategy* (ESS). An evolutionarily stable strategy cannot be invaded by any nearby strategy. This means that, under our assumption of small mutation steps, an ESS in a monomorphic population cannot be invaded at all. For any evolutionarily stable x^*, the vertical line $y = x^*$ on the pairwise invasibility plot will pass only through regions where $s_x(y) < 0$.

We say that x^* is locally *convergence stable* "if a population of a nearby phenotype can be invaded by mutants that are even closer to x^* – that is, if $s_x(y) > 0$ for $x < y < x^*$ and $x^* < y < x$" [10]. From the pairwise invasibility plot, then, we can conclude that x^* is convergence stable if, at $x = x^*$, $s_x(y) > 0$ above and to the left of the line $y = x$ as well as below and to the right of it. Since x^* is the point where "the sign of [the selection gradient] changes from positive to negative, $\left[\frac{\partial s_x(y)}{\partial y}\big|_{y=x}\right]$ is a (locally) decreasing function of x" [10]. Therefore, it holds that at a convergence stable x^*,

$$\frac{d}{dx}\left[\frac{\partial s_x(y)}{\partial y}\Big|_{y=x}\right]\Bigg|_{y=x=x^*} = \frac{\partial^2 s_x(y)}{\partial x \partial y}\Big|_{y=x=x^*} + \frac{\partial^2 s_x(y)}{\partial y^2}\Big|_{y=x=x^*} < 0.$$

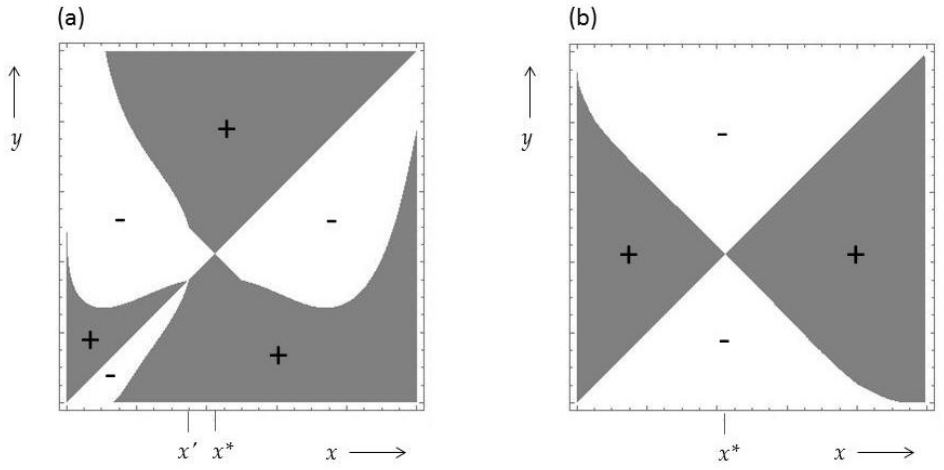

Figure 1. Examples of pairwise invasibility plots. In **(a)**, the invasion fitness $s_{x^*}(y)$ is positive for all values of y. Thus, the singular strategy x^* is a fitness minimum and can be invaded by all nearby strategies. Furthermore, as there is a (-) above and to the left (and below and to the right) of the diagonal at $x = x^*$, x^* is not convergence stable. Slightly to the left of x^*, there is a second singularity, x'. It is locally invasible from below but not from above and is thus neither a fitness maximum nor a fitness minimum. As $s_{x'}(y)$ is positive above-left and below-right of the diagonal, x' is convergence stable. In **(b)**, $s_{x^*}(y) < 0$ for all nearby y, and thus the singularity cannot be invaded. It is an ESS. As there is a (+) above and to the left (and below and to the right) of the diagonal at $x = x^*$, x^* is also convergence stable. Note that in both **(a)** and **(b)**, all strategies other than x^* can be invaded by some (but not all) values of y.

If, for a particular resident-mutant strategy pair (x, y), both $s_x(y) > 0$ and $s_y(x) > 0$, we say that x and y can *mutually invade*. As the mutant and resident each have a positive growth rate when rare in the other's presence, it is possible for the mutant population to flourish without replacing the resident. To visualize where mutual invasion may occur, we simply superimpose the PIPs of $s_y(x)$ and $s_x(y)$ to form a *mutual invasibility plot* (MIP). Regions where both of these functions are positive are those in which coexistence is possible.

If a strategy x^* is singular and convergence stable but not evolutionarily stable, a phenomenon known as *evolutionary branching* takes place. Near x^*, the resident and mutant coexist not only on the ecological timescale, but also on the evolutionary one. In other words, the mutant invades and establishes itself as a second resident, rendering the population dimorphic in the long term.

Why does this happen? When the population is monomorphic, $s_x(y)$ is locally concave up $\left(\frac{\partial^2 s_x(y)}{\partial y^2}\Big|_{y=x=x^*} > 0\right)$ and takes its minimum value, $s_{x^*}(x^*) = 0$, at the singular non-ESS x^*. However, if a slight perturbation pushes the minimum of this curve below the horizontal axis, the invasion fitness will have two roots, one on either side of x^*. In this case, we denote the curve $s_{x_1,x_2}(y)$, where x_1 and x_2 are the roots (and thus the resident strategies of the dimorphic population). Accordingly, $s_{x_1,x_2}(x_1) = s_{x_1,x_2}(x_2) = 0$. Given that $s_{x_1,x_2}(y)$ is concave up, it is negative for values of y between the roots (closer to x^*) and positive for values more extreme than the roots (further from x^*). Any successfully invading mutant will replace the resident on the same side of x^* as itself, driving the two resident strategies further apart. Subsequent invasion and substitution events will only increase the distance between them, meaning that we will never return to the original monomorphic population state.

The opposite situation holds when x^* in the monomorphic population is an ESS. In this case, $s_x(y)$ is locally concave down and equal to zero at $y = x^*$. When slight perturbations in this system bring $s_{x_1,x_2}(x^*)$ above the horizontal access, strategies closer to the local maximum x^* (between the roots) have positive invasion fitness. This means that any dimorphism is ultimately temporary, and the population always evolves back to the monomorphic ESS x^*.

In summary, strategy x^* is an evolutionary branching point if and only if it fulfills the following three conditions:

1. x^* is singular: $\frac{\partial s_x(y)}{\partial y}\Big|_{y=x=x^*} = 0$.
2. x^* is convergence stable: $\frac{\partial^2 s_x(y)}{\partial x \partial y}\Big|_{y=x=x^*} + \frac{\partial^2 s_x(y)}{\partial y^2}\Big|_{y=x=x^*} < 0$.
3. x^* is not an ESS: $\frac{\partial^2 s_x(y)}{\partial y^2}\Big|_{y=x=x^*} > 0$.

Later on, we will use these conditions to locate branching points in the model that we present in the following sections.

2 The within-host dynamics

2.1 The single-strain model

To lay the groundwork for the within-host model of a single pathogen strain, we consider the relationship between two loci on the pathogen genome. The first locus is associated with the attribute affecting the pathogen's intrinsic growth rate. We assume that any non-neutral mutation at this locus is almost surely deleterious such that a mutant a of wild type A has a reduced growth rate compared to that of A. A second site on the genome codes for the probability that a pathogen of type A produces a mutant offspring of type a (and vice versa). We denote the forward (A to a) mutation probability μ_{Aa} and the back mutation probability μ_{aA}. Furthermore, we define x_A and x_a to be the concentrations of pathogens of type A and type a, respectively, within the host organism. The sum $x = x_A + x_a$ represents the total pathogen load in the host. These assumptions enable us to form the following model of within-host dynamics:

$$\begin{cases} \dot{x}_A = [(1-\mu_{Aa})\lambda_A(\mu_{Aa}) - \sigma_A]x_A + \mu_{aA}\lambda_a(\mu_{Aa})x_a - cxx_A \\ \dot{x}_a = [(1-\mu_{aA})\lambda_a(\mu_{Aa}) - \sigma_a]x_a + \mu_{Aa}\lambda_A(\mu_{Aa})x_A - cxx_a. \end{cases}$$

In these equations, the background death rate of type A is σ_A, and that of type a is σ_a. The competition coefficient c is the rate at which pathogens are lost through competition with one another for host resources. λ_A and λ_a represent the reproduction rates of the wild and mutated type, respectively. We take μ_{aA} to be infinitesimal such that $\mu_{aA} = \epsilon\mu_{Aa}$, where $\epsilon \to 0$. In practice, this means that λ_A and λ_a are functions of μ_{Aa}, as the biological mechanisms that govern accuracy determine both μ_{Aa} and μ_{aA}. As faithful replication is costly to the pathogen, we assume these to be increasing functions. We define the deleterious effect of mutation on reproduction to be $s : 0 < s \leq 1$, the percentage by which growth is reduced in mutants. We then observe that

$$\lambda_a(\mu_{Aa}) = k\lambda_A(\mu_{Aa}), \tag{1}$$

where $k := 1 - s$. Taking into account equation (1) and the assumption that μ_{aA} is infinitesimal, the within-host dynamics simplify to

$$\begin{cases} \dot{x}_A = [(1-\mu)\lambda(\mu) - \sigma_A]x_A - cxx_A & \text{(2a)} \\ \dot{x}_a = [k\lambda(\mu) - \sigma_a]x_a + \mu\lambda(\mu)x_A - cxx_a. & \text{(2b)} \end{cases}$$

As μ_{aA} is currently absent from the model, we abbreviate μ_{Aa} as simply μ. Furthermore, because $\lambda_a(\mu) = k\lambda_A(\mu)$, we can express system (2) solely in terms of λ_A, which we henceforth abbreviate as λ.

From equation (2a), we derive the equilibrium condition that either $\hat{x}_A = 0$ (trivially) or $\hat{x} = \frac{(1-\mu)\lambda(\mu)-\sigma_A}{c}$. As $x = x_A + x_a$, the non-trivial condition can alternatively be expressed as $\hat{x}_A = \hat{x} - \hat{x}_a = \frac{(1-\mu)\lambda(\mu)-\sigma_A}{c} - \hat{x}_a$.

Equation (2b) prescribes that $\hat{x} = \frac{[k\lambda(\mu)-\sigma_a]\hat{x}_a+\mu\lambda(\mu)\hat{x}_A}{c\hat{x}_a}$. Combining the conditions obtained from both equations, we see that system (2) has three equilibria $(\hat{x}_A, \hat{x}_a)$. The first, $(0,0)$, is trivial. The second, $(0, \frac{k\lambda(\mu)-\sigma_a}{c})$, is a mutant-only steady state. The third,

$$\hat{x}_A^* = \frac{(1-\mu)\lambda(\mu) - \sigma_A}{c}\left(1 - \frac{\mu\lambda(\mu)}{(1-k)\lambda(\mu) + \sigma_a - \sigma_A}\right) \tag{3a}$$

$$\hat{x}_a^* = \frac{(1-\mu)\lambda(\mu) - \sigma_A}{c}\left(\frac{\mu\lambda(\mu)}{(1-k)\lambda(\mu) + \sigma_a - \sigma_A}\right), \tag{3b}$$

is an interior equilibrium.

As the quantity

$$\frac{(1-\mu)\lambda(\mu) - \sigma_A}{c} =: \hat{x}(\mu) \tag{4}$$

represents the total number of pathogens present in the host at equilibrium,

the interior equilibrium exists and is biologically realistic only when

$$\sigma_A < (1-\mu)\lambda(\mu) \tag{5a}$$

and

$$0 < \frac{\mu\lambda(\mu)}{(1-k)\lambda(\mu) + \sigma_a - \sigma_A} < 1. \tag{5b}$$

Equation (5a) prescribes that $\hat{x}(\mu) > 0$, while (5b) requires that the relative frequencies of types A and a take values between 0 and 1. Whenever (5b) is satisfied, it holds that

$$k\lambda(\mu) - \sigma_a < (1-\mu)\lambda(\mu) - \sigma_A. \tag{6}$$

This indicates that the intrinsic growth rate of the wild type must be greater than the intrinsic growth rate of the mutated type in order for the interior equilibrium to have biological meaning.

To determine the stability of this equilibrium, we examine the eigenvalues of the Jacobian of system (2) evaluated at that point. The generic form of the Jacobian is

$$J(\hat{x}_A, \hat{x}_a) = \begin{pmatrix} (1-\mu)\lambda(\mu) - \sigma_A - c\hat{x}_a - 2c\hat{x}_A & -c\hat{x}_A \\ \mu\lambda(\mu) - c\hat{x}_a & k\lambda(\mu) - \sigma_a - c\hat{x}_A - 2c\hat{x}_a \end{pmatrix}.$$

After plugging in $\hat{x}_A^*$ and $\hat{x}_a^*$ from (3a) and (3b), we calculate the eigenvalues of the resulting matrix. They are

$$\rho_1 = \lambda(\mu)(\mu - 1) + \sigma_A$$
$$\rho_2 = \lambda(\mu)(\mu + k - 1) - \sigma_a + \sigma_A.$$

When both of these values are negative, the equilibrium is stable. This occurs precisely when the conditions described by inequalities (5a) and (5b) are fulfilled. Thus, the interior equilibrium is stable whenever it is present.

To determine the stability of the mutant-only equilibrium, we plug $\hat{x}_A = 0$ and $\hat{x}_a = \frac{k\lambda(\mu)-\sigma_a}{c}$ into the Jacobian and recover the eigenvalues

$$\rho_1{}' = \sigma_a - k\lambda(\mu)$$
$$\rho_2{}' = -[\lambda(\mu)(\mu + k - 1) - \sigma_a + \sigma_A].$$

Notice that $\rho_1{}'$ is negative whenever $\hat{x}_a > 0$. Notice further that $\rho_2{}' = -\rho_2$. This means that whenever the interior equilibrium is present, $\rho_2{}' > 0$, and so the mutant-only equilibrium is unstable. Because we have assumed μ_{aA} to be infinitesimal but not 0, pathogens of type A are produced infrequently when the system is in this steady state. Since the state is unstable, the few wild-type pathogens produced here, if able to invade, will drive the system to the interior equilibrium.

2.2 The double-strain model

We now introduce a mutant strain with forward mutation rate ν to our within-host dynamics. We assume that it is not a neutral mutant, that is, that $\mu \neq \nu$. This gives rise to the four-dimensional system

$$\begin{cases} \dot{x}_A = [(1-\mu)\lambda(\mu) - \sigma_A]x_A - c(x+y)x_A & \text{(7a)} \\ \dot{x}_a = [k\lambda(\mu) - \sigma_a]x_a + \mu\lambda(\mu)x_A - c(x+y)x_a & \text{(7b)} \\ \dot{y}_A = [(1-\nu)\lambda(\nu) - \sigma_A]y_A - c(x+y)y_A & \text{(7c)} \\ \dot{y}_a = [k\lambda(\nu) - \sigma_a]y_a + \nu\lambda(\nu)y_A - c(x+y)y_a. & \text{(7d)} \end{cases}$$

Here, pathogen death via competition for host resources is proportional to the total pathogen load, $x + y$. In order for both x_A and y_A to be present at equilibrium, it must hold that $\hat{x}+\hat{y} = \frac{(1-\mu)\lambda(\mu)-\sigma_A}{c}$ (as prescribed by equation (7a)) and that $\hat{x}+\hat{y} = \frac{(1-\nu)\lambda(\nu)-\sigma_A}{c}$ (as prescribed by equation (7c)). However, this generically does not hold, as $\mu \neq \nu$. This means that our model does not admit coexistence of multiple pathogen strains at equilibrium. What will happen, then, if a host infected with one strain is subsequently exposed to another?

We observe that $\dot{x}_A$ and $\dot{y}_A$ can be expressed as $\dot{x}_A = \zeta(\mu, E)x_A$ and $\dot{y}_A = \zeta(\nu, E)y_A$, where $\zeta(\gamma, E) = (1-\gamma)\lambda(\gamma) - \sigma_A - cE$ and $E = x + y$. When a pathogen with mutation rate γ equilibrates E at $\frac{(1-\gamma)\lambda(\gamma)-\sigma_A}{c}$, we say that $E = \hat{E}_\gamma$. ζ is decreasing in E, so given that $\zeta(\mu, \hat{E}_\mu) = 0$, if $\zeta(\nu, \hat{E}_\mu) > 0$,

then $\hat{E}_\mu < \hat{E}_\nu$ (i.e. $\frac{(1-\mu)\lambda(\mu)-\sigma_A}{c} < \frac{(1-\nu)\lambda(\nu)-\sigma_A}{c}$). In other words, strain ν has a positive growth rate in a host already carrying strain μ if and only if it equilibrates E at a higher level than strain μ. As such, whichever strain is characterized by a higher equilibrium pathogen load persists in the host, and the other is lost. This means that these within-host dynamics form an optimization model that maximizes

$$f(\gamma) = (1-\gamma)\lambda(\gamma), \tag{8}$$

where, as above, γ is the pathogen mutation rate.

3 The between-host dynamics

3.1 Preliminaries

To describe the spread of a single pathogen type within the host population, we turn to the following SI model:

$$\begin{cases} \dot{S} = b - \beta(\mu)SI - \delta S \\ \dot{I} = \beta(\mu)SI - [\alpha(\mu) + \delta]I. \end{cases}$$

Susceptible hosts (S) are born at constant rate b and die at per capita rate δ. Infected individuals (I) encounter and infect susceptibles at rate β, which is a function of the equilibrium pathogen load $\hat{x}(\mu)$ in equation (4). By extension, then, β can be defined directly as a function of μ itself. Infected individuals have increased mortality α (virulence), which similarly depends on μ (via $\hat{x}(\mu)$). We define and discuss α and β in more detail in later sections of this thesis. Note that this SI model does not permit recovery from the disease; that is, once a host individual becomes infected, that individual will carry the pathogen for life. Additionally, it is assumed that all hosts are born susceptible; there is no vertical transmission of the disease.

This system has two equilibria $(\hat{S}, \hat{I})$. The first, $\left(\frac{b}{\delta}, 0\right)$, is trivial. The second,

$$\hat{S}(\mu) := \frac{\alpha(\mu) + \delta}{\beta(\mu)} \tag{9a}$$

$$\hat{I}(\mu) := \frac{b}{\alpha(\mu) + \delta} - \frac{\delta}{\beta(\mu)}, \tag{9b}$$

is biologically meaningful only when $\frac{b}{\delta} > \frac{\alpha(\mu)+\delta}{\beta(\mu)}$. This constraint ensures not only that $\hat{I}(\mu)$ is positive, but also that $S_0 =: \frac{b}{\delta}$, the susceptible population density in the absence of any pathogen, is larger than $\hat{S}(\mu)$. It is algebraically equivalent to the condition for pathogen viability, which is that the basic reproductive number, $\mathscr{R}_0(\mu)$, must be greater than 1.

By definition, $\mathscr{R}_0$ is the expected number of secondary infections caused by each infected individual. It is calculated as the rate new infections arise times the average amount of time individuals spend in the infected state. In our model, this gives

$$\mathscr{R}_0(\mu) = \frac{b\beta(\mu)}{\delta(\alpha(\mu) + \delta)}. \tag{10}$$

To determine the stability of the interior equilibrium, we look to the Jacobian,

$$J(\hat{S}(\mu), \hat{I}(\mu)) = \begin{pmatrix} -\beta(\mu)\hat{I}(\mu) - \delta & -\beta(\mu)\hat{S}(\mu) \\ \beta(\mu)\hat{I}(\mu) & \beta(\mu)\hat{S}(\mu) - (\alpha(\mu) + \delta) \end{pmatrix},$$

evaluated at that point. Plugging in $\hat{S}(\mu) = \frac{\alpha(\mu)+\delta}{\beta(\mu)}$ to the bottom-right entry of this matrix, we see that the entry is equal to zero. Thus, the Jacobian simplifies to

$$J(\hat{S}(\mu), \hat{I}(\mu)) = \begin{pmatrix} -\beta(\mu)\hat{I}(\mu) - \delta & -\beta(\mu)\hat{S}(\mu) \\ \beta(\mu)\hat{I}(\mu) & 0 \end{pmatrix}.$$

From here, it is clear that the trace, $-\beta(\mu)\hat{I}(\mu) - \delta$, is always negative and that the determinant, $\beta(\mu)^2\hat{S}(\mu)\hat{I}(\mu)$, is always positive. This implies that the interior equilibrium is stable whenever it is present. The host population will reach it almost immediately on the long timescale of evolution, provided that the pathogen is viable.

To allow for the circulation of multiple varieties of pathogen in the host population, we initially assume cross-immunity between them. In other words, if a host carrying strain μ is subsequently exposed to strain ν, infection by the latter will not take place. From this assumption, we formulate the following model:

$$\begin{cases} \dot{S} = b - \beta(\mu)SI_\mu - \beta(\nu)SI_\nu - \delta S & \text{(11a)} \\ \dot{I}_\mu = \beta(\mu)SI_\mu - [\alpha(\mu) + \delta]I_\mu & \text{(11b)} \\ \dot{I}_\nu = \beta(\nu)SI_\nu - [\alpha(\nu) + \delta]I_\nu. & \text{(11c)} \end{cases}$$

From equation (11b), we see that in order for hosts infected with strain μ to be present at equilibrium, it must hold that $\hat{S} = \frac{\alpha(\mu)+\delta}{\beta(\mu)}$. Similarly, from equation (11c), we see that if hosts infected with strain ν are present at equilibrium, then $\hat{S} = \frac{\alpha(\nu)+\delta}{\beta(\nu)}$. As type ν is assumed to not be a neutral mutant of type μ, these two conditions cannot generically be satisfied simultaneously. Thus, at most one strain can persist in the host population at equilibrium, meaning this model does not admit steady coexistence of strains.

To determine which strain will win the between-host competition, we proceed as we did in section 2.2, where we showed that, at the within-host level, whichever strain maximizes the pathogen load goes to fixation, while the other is lost. We begin by observing that $\dot{I}_\mu$ and $\dot{I}_\nu$ can be expressed as $\dot{I}_\mu = \eta(\mu, E)I_\mu$ and $\dot{I}_\nu = \eta(\nu, E)I_\nu$, where $\eta(\gamma, E) = \beta(\gamma)E - [\alpha(\gamma) + \delta]$ and $E = S$. Here, $\hat{E}_\gamma := \frac{\alpha(\gamma)+\delta}{\beta(\gamma)}$ is the value that E takes when equilibrated by a pathogen with mutation rate γ.

η is increasing in E, so given that $\eta(\mu, \hat{E}_\mu) = 0$, if $\eta(\nu, \hat{E}_\mu) > 0$, then $\hat{E}_\nu < \hat{E}_\mu$ (i.e. $\frac{\alpha(\nu)+\delta}{\beta(\nu)} < \frac{\alpha(\mu)+\delta}{\beta(\mu)}$). This means that, in a host population in which strain μ circulates, strain ν can invade and replace μ if and only if it equilibrates the number of susceptible hosts at a lower level than strain μ. Therefore, these between-host dynamics form an optimization model that maximizes the inverse of $\hat{S}(\gamma)$,

$$g(\gamma) = \frac{\beta(\gamma)}{\alpha(\gamma) + \delta}.$$

As $\mathscr{R}_0(\gamma) = \frac{b}{\delta} g(\gamma)$, this is tantamount to maximizing $\mathscr{R}_0(\gamma)$. Further expla-

nation (and a nice example) of optimizing a pathogen at the between-host level is given in Corollary 1 of Theorem 1 in [17].

Notice that the population-level winner – the strain that maximizes g – is determined independently of the within-host dynamics. This is due to our assumption of cross-immunity between strains, under which the host-level "winner" is simply the strain that infects the host first. Here, there is no within-host selection to influence the population-wide competition.

3.2 The superinfection model

We now allow for the possibility that hosts infected by one strain of the pathogen can be reinfected if exposed to the second strain. We assume that the within-host dynamics operate on a timescale faster than the epidemiological one, meaning that it takes the pathogen load in an individual much less time to reach $\hat{x}$ or $\hat{y}$ than it takes the population to stabilize at $\hat{S}$ and $\hat{I}$. As there can be no coexistence of strains within a host, the mutant strain, upon entering a host infected by the resident, either does not invade or does so and immediately substitutes that resident. Following Boldin and Diekmann (2008), we formulate the superinfection model as follows:

$$\begin{cases} \dot{S} = b - \beta(\mu)SI_\mu - \beta(\nu)SI_\nu - \delta S & \text{(12a)} \\ \dot{I}_\mu = \beta(\mu)SI_\mu - [\alpha(\mu) + \delta]I_\mu + \Phi(\nu,\mu)I_\mu I_\nu & \text{(12b)} \\ \dot{I}_\nu = \beta(\nu)SI_\nu - [\alpha(\nu) + \delta]I_\nu + \Phi(\mu,\nu)I_\mu I_\nu. & \text{(12c)} \end{cases}$$

The superinfection function, Φ, is defined as

$$\Phi(\mu, \nu) = \beta(\nu)\phi(\mu, \nu) - \beta(\mu)\phi(\nu, \mu), \tag{13}$$

where $\phi(\mu, \nu)$ is the probability that a pathogen with mutation rate ν, upon transmission to a host carrying a pathogen with mutation rate μ, will eliminate that resident and take over the host. More specifically, we can express ϕ as a function of f from equation (8): $\phi(\mu, \nu) = \Psi(f(\mu), f(\nu))$. As we determined in section 2.2, if $f(\mu) > f(\nu)$, then strain ν cannot increase its population size in a host already equilibrated with strain μ. In the case of

a neutral mutant (one with mutation rate $\nu : \nu = \mu$), the resident and invading strains have identical growth rates. Because we assume a very large within-host pathogen population, the probability that this initially rare neutral mutant manages to proliferate and replace the resident is negligible. As such,

$$\Psi(f(\mu), f(\nu)) = 0 \text{ whenever } f(\mu) \geq f(\nu).$$

We now calculate the invasion fitness of any mutant ν. It is

$$r_\mu(\nu) = \beta(\nu)\hat{S}(\mu) - [\alpha(\nu) + \delta] + \hat{I}(\mu)\Phi(\mu, \nu),$$

where $\hat{S}(\mu)$ and $\hat{I}(\mu)$ are as defined in (9a) and (9b). The first two terms of the right-hand side are equal to the invasion fitness in the absence of superinfection, which is

$$s_\mu(\nu) = \beta(\nu)\hat{S}(\mu) - [\alpha(\nu) + \delta]. \tag{14}$$

Thus,

$$r_\mu(\nu) = s_\mu(\nu) + \hat{I}(\mu)\Phi(\mu, \nu). \tag{15}$$

Before we can identify singular strategies in this model, we must explicitly define α, β, λ and ϕ. In the coming sections, we examine how singularities and their stability depend on the precise form of the superinfection function.

3.2.1 The jump case of the superinfection function

If we assume that the pathogen's within-host dynamics are deterministic, we can construct the simple, piecewise superinfection function given by

$$\phi(\mu, \nu) = \begin{cases} 1 & \text{if } f(\nu) > f(\mu) \\ 0 & \text{otherwise.} \end{cases} \tag{16}$$

By this definition, all invading strains ν that satisfy $f(\nu) > f(\mu)$ hold exactly

the same advantage over the resident; it makes no difference *how much* better the invader is. Because of the jump discontinuity at $\mu = \nu$ (for which this case is named), we cannot differentiate $r_\mu(\nu)$ to find singularities. Nevertheless, the simplicity of this superinfection function allows us to characterize singular strategies via alternative means. Our approach is to prove that, with the above definition in place, a strategy is optimal at the between-host level if and only if it is also optimal at the within-host level.

First, consider a pathogen strain with mutation rate μ^*, a within-host optimal strategy. Since μ^* maximizes f, for any $\mu \neq \mu^*$, it holds that $f(\mu) < f(\mu^*)$. Furthermore, $\phi(\mu^*, \mu) = 0$ and $\phi(\mu, \mu^*) = 1$, which gives $\Phi(\mu^*, \mu) = -\beta(\mu^*)$. As we operate on the assumption that mutation occurs in small steps (and thus that $\mu = \mu^* + \epsilon$), it holds that $s_{\mu^*}(\mu) = O(\epsilon)$. We can therefore neglect this term from our calculation of $r_{\mu^*}(\mu)$, which yields $r_{\mu^*}(\mu) = \hat{I}(\mu^*)\Phi(\mu^*, \mu) = -\beta(\mu^*)\hat{I}(\mu^*)$. As $r_{\mu^*}(\mu)$ is always negative in the neighborhood of μ^*, this strategy cannot be invaded and so is optimal at the host population level.

Now, suppose there exists a between-host optimal strategy μ' and another strategy μ'' such that $\mu', \mu'' \neq \mu^*$ and $f(\mu') < f(\mu'') < f(\mu^*)$. It follows that $\phi(\mu', \mu'') = 1$ and $\phi(\mu'', \mu') = 0$, so $\Phi(\mu', \mu'') = \beta(\mu'')$. Again recalling the assumption of small mutation steps, we observe that $\mu' = \mu'' + \epsilon$ and $s_{\mu'}(\mu'') = O(\epsilon)$. Using these facts, we calculate that $r_{\mu'}(\mu'') = \beta(\mu'')\hat{I}(\mu')$. As $r_{\mu'}(\mu'') > 0$, any μ'' that fulfills $f(\mu') < f(\mu'')$ has a positive probability of invading a resident population with mutation rate μ'. But this contradicts the assumption that μ' is optimal at the between-host level. As such, there cannot exist a between-host optimal strategy that is not also a within-host optimal strategy. This means that μ^* is the only population-level optimum.

Because the above arguments show that μ^* cannot be invaded by any other strategy, we conclude that it is a fitness maximum and so an evolutionarily stable singularity.

3.2.2 The mechanistic case of the superinfection function

Because mutant parasites are assumed to be rare at the moment they enter the host, their initial growth in the resident population can be heavily influenced by demographic stochasticity. Thus, we now relax the assumption that the pathogen's within-host dynamics are deterministic, and we derive

the following superinfection function mechanistically.

We begin by modeling the growth of inocula of one strain's wild and mutated variants as a multi-type birth-death process. From this, we recover the probability that the initial inoculum of an invading strain is immediately cleared upon entering a host carrying another strain. Subtracting this value from one, we arrive at the mechanistic definition of ϕ for which this case is named.

As steady coexistence of traits within a host is impossible for nearly all combinations of μ and ν, when mutant strain ν invades a host infected with resident strain μ, it enters a monomorphic population of μ. At the moment ν is introduced, the within-host population is at its stable interior equilibrium value, $\hat{x}(\mu)$. The pathogen load of strain ν is $y = O(\epsilon)$. Thus, $x + y \approx \hat{x}(\mu)$, and so the dynamics describing the growth of strain ν within the host are

$$\begin{cases} \dot{y}_A = [(1-\nu)\lambda(\nu) - \sigma_A]y_A - c\hat{x}(\mu)y_A \\ \dot{y}_a = [k\lambda(\nu) - \sigma_a]y_a + \nu\lambda(\nu)y_A - c\hat{x}(\mu)y_a. \end{cases}$$

Plugging in the value of $\hat{x}(\mu)$ yields

$$\begin{cases} \dot{y}_A = [(1-\nu)\lambda(\nu) - \sigma_A]y_A - [(1-\mu)\lambda(\mu) - \sigma_A]y_A & \text{(17a)} \\ \dot{y}_a = [k\lambda(\nu) - \sigma_a]y_a + \nu\lambda(\nu)y_A - [(1-\mu)\lambda(\mu) - \sigma_A]y_a. & \text{(17b)} \end{cases}$$

System (17) provides the information we need to lay the groundwork for our multi-type birth-death analysis of mutant strain ν's growth when present in finite numbers. First, we identify all the classes of individuals (so-called i-states) present in this model. There are two: wild-type individuals (A) and mutated individuals (a). Next, we identify the per capita rates of entry to and exit from each state due to the biological processes described in section 2.1. Figure 2 below presents a list of all possible events (i-processes) that can occur in the lifetimes of A- and a-type individuals. It is assumed that there is at most one event per infinitesimal time step.

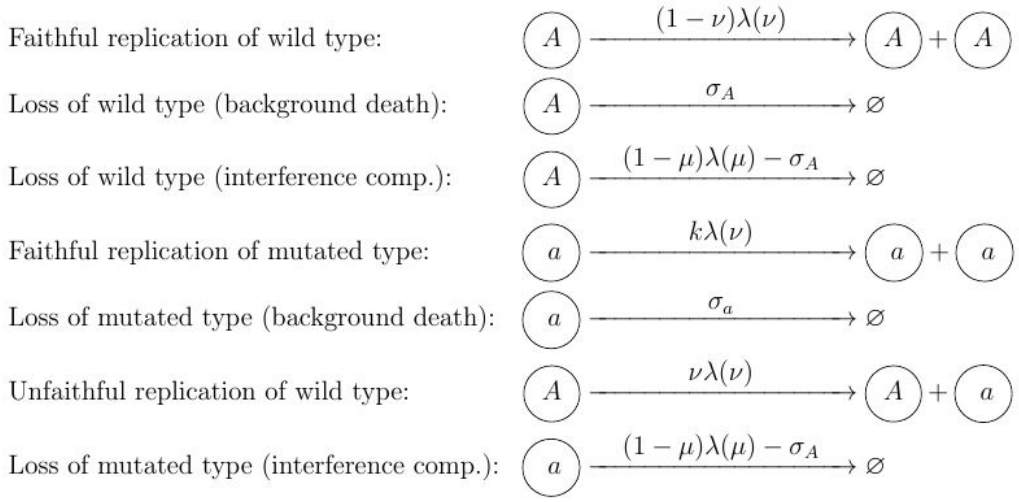

Figure 2. i-processes. The term on the left-hand side of each arrow represents the individual undergoing a life event. The term above the arrow indicates the per capita rate at which that event is expected to occur. Individuals present after the event (if any) appear to the right of the arrow. The symbol $\varnothing$ indicates that no live individuals remain.

At the population level, the number of invading pathogens changes according to the frequencies of the life events above and according to the principle of mass action. We define the p-state (the distribution of the two individual types in this population) as $\{(Y_A(t), Y_a(t))\}_{t\geq 0} \in \{0, 1, 2, ...\}^2$, where t represents the time since invasion and $t = 0$ is the moment of invasion. Table 1 interprets the i-level processes above in the context of population-level changes that increase or decrease the total number of wild or mutated invading pathogens in the host.

Table 1. p-level state changes.

Event	$\Delta Y_A, \Delta Y_a$	Population rate
Faithful replication of wild type	$+1, 0$	$(1-\nu)\lambda(\nu)Y_A$
Loss of wild type (background death)	$-1, 0$	$\sigma_A Y_A$
Loss of wild type (interference comp.)	$-1, 0$	$[(1-\mu)\lambda(\mu) - \sigma_A]Y_A$
Faithful replication of mutated type	$0, +1$	$k\lambda(\nu)Y_a$
Loss of mutated type (background death)	$0, -1$	$\sigma_a Y_a$
Unfaithful replication of wild type	$0, +1$	$\nu\lambda(\nu)Y_A$
Loss of mutated type (interference comp.)	$0, -1$	$[(1-\mu)\lambda(\mu) - \sigma_A]Y_a$

We define the probability that the population is in a particular state at a given moment as $P_{n,m}(t) = Prob[(Y_A(t), Y_a(t)) = (n, m)]$, where n and m are the number of wild-type and mutated individuals, respectively. As $P_{n,m}(t)$ is a probability, it must hold that $0 \leq P_{n,m}(0) \leq 1$ and that $\sum_{n,m \geq 0} P_{n,m}(0) = 1$.

The probability that the $n+m$ individuals currently alive (and any descendants they may produce) all eventually go extinct is denoted $E_{n,m}$. Because individuals do not interact with each other in a linear birth-death process, their behavior is independent of one another's, and so $E_{n,m} = (E_{1,0})^n (E_{0,1})^m$. Note that $E_{0,0} = 1$ trivially.

Using the rates in table 1, we can proceed event by event to construct $\frac{dP_{n,m}}{dt}$ as follows:

$$\begin{aligned}
\frac{dP_{n,m}}{dt} =& (1-\nu)\lambda(\nu)(n-1)P_{n-1,m} - (1-\nu)\lambda(\nu)nP_{n,m} \\
&+ (1-\mu)\lambda(\mu)(n+1)P_{n+1,m} - (1-\mu)\lambda(\mu)nP_{n,m} \\
&+ k\lambda(\nu)(m-1)P_{n,m-1} - k\lambda(\nu)mP_{n,m} \\
&+ [(1-\mu)\lambda(\mu) - \sigma_A + \sigma_a](m+1)P_{n,m+1} - [(1-\mu)\lambda(\mu) - \sigma_A + \sigma_a]mP_{n,m} \\
&+ \nu\lambda(\nu)nP_{n,m-1} - \nu\lambda(\nu)nP_{n,m}.
\end{aligned}$$

Simplifying yields

$$\begin{aligned}\frac{dP_{n,m}}{dt} =&(1-\nu)\lambda(\nu)[(n-1)P_{n-1,m} - nP_{n,m}] \\ &+ (1-\mu)\lambda(\mu)[(n+1)P_{n+1,m} - nP_{n,m}] \\ &+ k\lambda(\nu)[(m-1)P_{n,m-1} - mP_{n,m}] \\ &+ [(1-\mu)\lambda(\mu) - \sigma_A + \sigma_a][(m+1)P_{n,m+1} - mP_{n,m}] \\ &+ \nu\lambda(\nu)[nP_{n,m-1} - nP_{n,m}].\end{aligned} \tag{18}$$

Now, suppose that upon exposure to pathogen strain ν, the host receives exactly one inoculum, which is either an A- or a-type individual. This individual and its descendants comprise a so-called clan that will either persist or go extinct as time goes to infinity. In other words, the infection established by this initial inoculum will either proliferate in the host or die out. If the inoculum is of type A, the probability that its clan will eventually go extinct is $E_{1,0}$. Likewise, if it is of type a, the probability that its clan will eventually go extinct is $E_{0,1}$. Conceptually, we construct $E_{1,0}$ as follows:

$$\begin{aligned}E_{1,0} =&Prob[\text{Next event is death of } A] \cdot E_{0,0} \\ &+ Prob[\text{Next event is faithful reproduction of } A] \cdot E_{2,0} \\ &+ Prob[\text{Next event is unfaithful reproduction of } A] \cdot E_{1,1}.\end{aligned}$$

Similarly, we construct $E_{0,1}$ as

$$\begin{aligned}E_{0,1} =&Prob[\text{Next event is death of } a] \cdot E_{0,0} \\ &+ Prob[\text{Next event is faithful reproduction of } a] \cdot E_{0,2}.\end{aligned}$$

Recalling that $E_{n,m} = (E_{1,0})^n (E_{0,1})^m$, we see that in the equations above, $E_{2,0} = {E_{1,0}}^2$, $E_{1,1} = E_{1,0} \cdot E_{0,1}$, and $E_{0,2} = {E_{0,1}}^2$. Thus,

$$\begin{aligned}E_{1,0} =&Prob[\text{Next event is death of } A] \cdot E_{0,0} \\ &+ Prob[\text{Next event is faithful reproduction of } A] \cdot {E_{1,0}}^2 \\ &+ Prob[\text{Next event is unfaithful reproduction of } A] \cdot E_{1,0} \cdot E_{0,1},\end{aligned} \tag{19}$$

and

$$\begin{aligned}E_{0,1} =&Prob[\text{Next event is death of } a] \cdot E_{0,0} \\ &+ Prob[\text{Next event is faithful reproduction of } a] \cdot {E_{0,1}}^2.\end{aligned} \tag{20}$$

Note that because μ_{aA} is infinitesimal but nevertheless positive, the clan of an invader of type a will produce rare A-type individuals. However, as this process occurs too infrequently to consider explicitly in (17), the event of unfaithful reproduction of a does not occur in the formulation of $E_{0,1}$. Nevertheless, if ν is able to invade with an initial inoculum of type a, as soon as the clan spawns an A-type offspring, the host will be equilibrated as in (3) (with ν, not μ, as the resident).

Bearing this in mind, we now begin the calculation of $E_{1,0}$ and $E_{0,1}$. To calculate $Prob$[Next event is death of A], we divide the per capita death rate of A-type individuals by the sum of the per capita rates of all changes that an A-type individual can undergo. Taking these rates from figure 2, we find

$$\begin{aligned} Prob[\text{Next event is death of } A] =& \frac{A \text{ dies (background)} + A \text{ dies (competition)}}{\text{Sum of per capita rates of all changes } A \text{ can undergo}} \\ =& \frac{\sigma_A + [(1-\mu)\lambda(\mu) - \sigma_A]}{(1-\nu)\lambda(\nu) + \sigma_A + [(1-\mu)\lambda(\mu) - \sigma_A] + \nu\lambda(\nu)} \\ =& \frac{(1-\mu)\lambda(\mu)}{\lambda(\nu) + (1-\mu)\lambda(\mu)}. \end{aligned}$$

The remaining probabilities are calculated similarly and are then plugged into (19) and (20). This yields the following definitions of $E_{1,0}$ and $E_{0,1}$:

$$E_{1,0} = \frac{(1-\mu)\lambda(\mu)}{\lambda(\nu) + (1-\mu)\lambda(\mu)} E_{0,0} + \frac{(1-\nu)\lambda(\nu)}{\lambda(\nu) + (1-\mu)\lambda(\mu)} {E_{1,0}}^2 + \frac{\nu\lambda(\nu)}{\lambda(\nu) + (1-\mu)\lambda(\mu)} E_{1,0}E_{0,1}$$

$$E_{0,1} = \frac{k\lambda(\nu)}{k\lambda(\nu) + \sigma_a + (1-\mu)\lambda(\mu) - \sigma_A} {E_{0,1}}^2 + \frac{\sigma_a + (1-\mu)\lambda(\mu) - \sigma_A}{k\lambda(\nu) + \sigma_a + (1-\mu)\lambda(\mu) - \sigma_A} E_{0,0}.$$

Recalling that $E_{0,0} = 1$ and factoring, the above simplify to

$$E_{1,0} = \frac{1}{\lambda(\nu) + (1-\mu)\lambda(\mu)} \left[(1-\mu)\lambda(\mu) + (1-\nu)\lambda(\nu){E_{1,0}}^2 + \nu\lambda(\nu)E_{1,0}E_{0,1}\right]$$

$$E_{0,1} = \frac{1}{k\lambda(\nu) + \sigma_a + (1-\mu)\lambda(\mu) - \sigma_A} \left[k\lambda(\nu){E_{0,1}}^2 + \sigma_a + (1-\mu)\lambda(\mu) - \sigma_A\right].$$

To ease the algebra on the coming pages, we define the following:

$$
\begin{aligned}
B &:= (1-\mu)\lambda(\mu) \\
C &:= (1-\nu)\lambda(\nu) \\
D &:= \nu\lambda(\nu) \\
G &:= k\lambda(\nu) \\
H &:= \sigma_a + (1-\mu)\lambda(\mu) - \sigma_A.
\end{aligned}
$$

Substituting these values into the equations for $E_{1,0}$ and $E_{0,1}$, we obtain the two-dimensional system

$$
\begin{cases}
E_{1,0} = \dfrac{1}{B+C+D}\left[B + C{E_{1,0}}^2 + DE_{1,0}E_{0,1}\right] & \text{(22a)} \\
E_{0,1} = \dfrac{1}{G+H}\left[G{E_{0,1}}^2 + H\right]. & \text{(22b)}
\end{cases}
$$

Solving equation (22b) for $E_{0,1}$, we find that $E_{0,1} = \dfrac{1 \pm \sqrt{1 - \left(2\frac{G}{G+H}\right)\left(2\frac{H}{G+H}\right)}}{2\frac{G}{G+H}}$. Note that G is always positive by definition, and recall from (5a) that $(1-\mu)\lambda(\mu) - \sigma_A > 0$ whenever $x = \hat{x}(\mu)$. This means that H, too, is positive here. By defining $p := \frac{G}{G+H}$, we can express $E_{0,1}$ as a function of a single variable, namely

$$
E_{0,1} := h(p) = \frac{1 \pm \sqrt{1 - 4p(1-p)}}{2p}
$$

for $p \in (0,1)$. Regrouping the terms in the discriminant yields

$$
h(p) = \frac{1 \pm \sqrt{(1-2p)^2}}{2p} = \frac{1 \pm |1-2p|}{2p}.
$$

The term $1-2p$ is positive when $0 < p < 1/2$ and negative when $1/2 < p < 1$. This fact gives rise to the following three cases.

Case 1 $0 < p < 1/2$. As the modulus $|1-2p|$ is positive, $h(p) = \frac{1 \pm (1-2p)}{2p}$. Thus, the negative root is $h_-(p) = \frac{1-(1-2p)}{2p} = 1$, and the positive root is $h_+(p) = \frac{1+(1-2p)}{2p} = \frac{1-p}{p}$. Because $p < 1/2$, $h_+(p) > 1$.

Case 2 $p = 1/2$. Here, the modulus is equal to 0, and $h_+(\frac{1}{2}) = h_-(\frac{1}{2}) = 1$.

Case 3 $1/2 < p < 1$. Now, $|1 - 2p| = 2p - 1$, and so $h(p) = \frac{1 \pm (2p-1)}{2p}$. In this case, $h_-(p) = \frac{1-(2p-1)}{2p} = \frac{1-p}{p}$ and $h_+(p) = 1$. Because $1/2 < p < 1$, $0 < h_-(p) < 1$.

Combining our conclusions from all three cases, we readily see that it always holds that $0 < h_-(p) \leq 1$ and that $h_+(p) \geq 1$. As $h(p)$ is a probability, only $h_-(p)$ assigns it realistic values for all p. Furthermore, by Theorem 6.5.1 of [13], we know that because both $h_+(p)$ and $h_-(p)$ are greater than zero, the probability of eventual extinction is the smaller of the two. Thus, we discard $h_+(p)$ and take $h(p) = h_-(p)$. We may now conclude that the negative root is the one that will preserve the condition that $0 \leq E_{0,1} \leq 1$. Therefore,

$$\begin{aligned} E_{0,1} &= \frac{1 - \sqrt{1 - \left(2\frac{G}{G+H}\right)\left(2\frac{H}{G+H}\right)}}{2\frac{G}{G+H}} = \frac{1 - \sqrt{1 - \frac{4GH}{(G+H)^2}}}{2\frac{G}{G+H}} \\ &= \frac{1 - \sqrt{\frac{(G+H)^2 - 4GH}{(G+H)^2}}}{2\frac{G}{G+H}} = \frac{1 - \sqrt{\frac{(G-H)^2}{(G+H)^2}}}{2\frac{G}{G+H}} = \frac{1 - \frac{|G-H|}{G+H}}{2\frac{G}{G+H}} \\ &= \frac{G + H - |G - H|}{2G}. \end{aligned}$$

Note that when $0 < p < \frac{1}{2}$ (in case 1), it holds that

$$\begin{aligned} \frac{2G}{G+H} < 1 \leftrightarrow G < H &\leftrightarrow k\lambda(\nu) - \sigma_a < (1-\mu)\lambda(\mu) - \sigma_A \\ &\leftrightarrow k\lambda(\nu) - \sigma_a - [(1-\mu)\lambda(\mu) - \sigma_A] < 0, \end{aligned}$$

which means that the intrinsic growth rate of any a-type initial inoculum is negative. As such, we know that the clan of this inoculum (if even established) is automatically bound for extinction whenever $G < H$.

It now remains to solve for $E_{1,0}$. Equation (22a) prescribes that

$$g(E_{1,0}) = \frac{C{E_{1,0}}^2}{B + C + D} + \left[\frac{DE_{0,1}}{B + C + D} - 1\right] E_{1,0} + \frac{B}{B + C + D} = 0. \quad (23)$$

Using the quadratic formula to solve for $E_{1,0}$, we find

$$E_{1,0} = \frac{1 - \frac{DE_{0,1}}{B+C+D} \pm \sqrt{\left[\frac{DE_{0,1}}{B+C+D} - 1\right]^2 - \frac{4BC}{(B+C+D)^2}}}{\frac{2C}{B+C+D}}$$
$$= \frac{B + C + D(1 - E_{0,1}) \pm \sqrt{[D(E_{0,1} - 1) - B - C]^2 - 4BC}}{2C}. \quad (24)$$

To determine which of $E_{1,0-}$ (the negative root) and $E_{1,0+}$ (the positive root) will satisfy the condition that $0 \leq E_{1,0} \leq 1$, we consider the following two cases.

Case 1 $0 \leq E_{0,1} < 1$. We examine the qualitative properties of g at $E_{1,0} = 0$ and at $E_{1,0} = 1$. First, we calculate the first and second derivatives of this function with respect to $E_{1,0}$. They are

$$g'(E_{1,0}) = \frac{2C}{B + C + D} E_{1,0} + \frac{DE_{0,1}}{B + C + D} - 1$$
$$g''(E_{1,0}) = \frac{2C}{B + C + D}.$$

Because g'' is always positive, we know that g, a parabola, is concave up. At the origin, $g(0) = \frac{B}{B+C+D} > 0$ and $g'(0) = \frac{DE_{0,1}}{B+C+D} - 1 < 0$. Combining the facts that $g(0) > 0$, $g'(0) < 0$ and $g''(0) > 0$, we conclude that both $E_{1,0-}$ and $E_{1,0+}$ are positive. Then, we compute $g(1) = \frac{B+C+DE_{0,1}}{B+C+D} - 1$. As $0 \leq E_{0,1} < 1$, $g(1)$ is strictly negative. This means that $E_{1,0-}$ always lies between 0 and 1 and that $E_{1,0+}$ is always greater than 1.

Case 2 $E_{0,1} = 1$. To determine which root will never exceed one, we compare the values that each assigns $E_{1,0}$ when $B > C$, when $B = C$, and when $B < C$. Note that when $E_{0,1} = 1$, the definition of $E_{1,0}$ in (24) simplifies to

$$E_{1,0} = \frac{B + C \pm \sqrt{(B+C)^2 - 4BC}}{2C} = \frac{B + C \pm \sqrt{(B-C)^2}}{2C} = \frac{B + C \pm |B - C|}{2C}. \quad (25)$$

Case 2.1 The positive root: $E_{1,0+} = \frac{B+C+|B-C|}{2C}$. When $B > C$, $E_{1,0+} = \frac{B+C+(B-C)}{2C} = \frac{2B}{2C} > 1$. When $B \leq C$, $E_{1,0+} = \frac{B+C+(C-B)}{2C} = \frac{2C}{2C} = 1$. Thus, $E_{1,0+}$ always takes a value greater than or equal to one.

Case 2.2 The negative root: $E_{1,0-} = \frac{B+C-|B-C|}{2C}$. When $B \geq C$, $E_{1,0-} = \frac{B+C-(B-C)}{2C} = \frac{2C}{2C} = 1$. When $B < C$, $E_{1,0-} = \frac{B+C-(C-B)}{2C} = \frac{2B}{2C} < 1$. Thus, $E_{1,0-}$ always takes a value less than or equal to one.

We thus conclude that when $E_{0,1} = 1$, it holds that $0 < E_{1,0-} \leq 1$ and $E_{1,0+} \geq 1$.

Because $B = (1-\mu)\lambda(\mu) = f(\mu)$ and $C = (1-\nu)\lambda(\nu) = f(\nu)$, our findings in case 2.2 have a clear biological interpretation: When $f(\mu) \geq f(\nu)$, the mutant – a weaker within-host strategy than the resident – faces certain extinction. Only when $f(\mu) < f(\nu)$ does the mutant stand a chance at successful invasion.

Our combined conclusions from case 1 and case 2 reveal that $0 < E_{1,0-} \leq 1$ and $E_{1,0+} \geq 1$ regardless of the value of $E_{0,1}$. Again by Theorem 6.5.1 of [13], this means that $E_{1,0-}$ is the correct value for the probability of eventual extinction, and so

$$E_{1,0} = \frac{B + C + \frac{D(G-H+|G-H|)}{2G} - \sqrt{[\frac{D(H-G-|G-H|)}{2G} - B - C]^2 - 4BC}}{2C}. \quad (26)$$

When $E_{0,1} = 1$, this simplifies to

$$E_{1,0} = \frac{B + C - |B - C|}{2C} = \frac{f(\mu) + f(\nu) - |f(\mu) - f(\nu)|}{2f(\nu)}. \quad (27)$$

Now that we have explicit values for $E_{0,1}$ and $E_{1,0}$, we are nearly ready to present our mechanistic definition of ϕ, which we conceptualize as follows:

$$\begin{aligned}\phi(\mu,\nu) = 1 - [&Prob(\text{Initial inoculum is type } A)\cdot E_{1,0}\\ &+ Prob(\text{Initial inoculum is type } a)\cdot E_{0,1}].\end{aligned}$$

Note that the probability of the initial inoculum being of the wild (mutated) type is equal to the relative frequency of A (a) at equilibrium. Fortunately, we can recover these frequencies from system (3), which gives

$$\begin{aligned}Prob(\text{Initial inoculum is type } A) &= 1 - F(\nu)\\ Prob(\text{Initial inoculum is type } a) &= F(\nu),\end{aligned}$$

where

$$F(\nu) := \frac{\nu\lambda(\nu)}{(1-k)\lambda(\nu) + \sigma_a - \sigma_A}. \tag{28}$$

Armed with this information, we can now state the full definition of ϕ. It is

$$\begin{aligned}&\phi(\mu,\nu) =\\ &1 - \left(1 - \frac{\nu\lambda(\nu)}{(1-k)\lambda(\nu) + \sigma_a - \sigma_A}\right)\\ &\cdot \frac{B + C + \frac{D(G-H+|G-H|)}{2G} - \sqrt{[\frac{D(H-G-|G-H|)}{2G} - B - C]^2 - 4BC}}{2C}\\ &- \frac{\nu\lambda(\nu)}{(1-k)\lambda(\nu) + \sigma_a - \sigma_A}\cdot\frac{G + H - |G-H|}{2G}.\end{aligned} \tag{29}$$

Recall that if $G - H > 0$, then $E_{0,1} = \frac{G+H-G+H}{2G} = \frac{H}{G}$, which is less than one whenever the inequality holds. If $G - H < 0$, then $E_{0,1} = \frac{G+H-(H-G)}{2G} = 1$. This means that any initial invader of type a is bound for extinction unless $H < G$, that is, unless

$$(1-\mu)\lambda(\mu) - \sigma_A < k\lambda(\nu) - \sigma_a. \tag{30}$$

From system (2), we readily see that this condition would be satisfied if and only if the intrinsic growth rate of the resident's wild type were lower than that of the mutant's mutated type. However, recall from inequality (6) that, because the resident is at its stable interior equilibrium, it holds that $k\lambda(\mu) - \sigma_a < (1-\mu)\lambda(\mu) - \sigma_A$. Since we have assumed small mutation steps, $|\mu - \nu| < \delta$ for δ very small, and so $\lambda(\mu) \approx \lambda(\nu)$. As such, $k\lambda(\nu) - \sigma_a < (1-\mu)\lambda(\mu) - \sigma_A$, which means that (30) cannot be satisfied. We may thus conclude that, given a monomorphic resident population, $E_{0,1}$ is always equal to one, and so $E_{1,0} = \frac{f(\mu)+f(\nu)-|f(\mu)-f(\nu)|}{2f(\nu)}$ (as shown in (27)). These facts simplify the superinfection function to

$$\begin{aligned}\phi(\mu,\nu) = \\ 1 - \left(1 - \frac{\nu\lambda(\nu)}{(1-k)\lambda(\nu) + \sigma_a - \sigma_A}\right) \cdot \frac{f(\mu) + f(\nu) - |f(\mu) - f(\nu)|}{2f(\nu)} \\ - \frac{\nu\lambda(\nu)}{(1-k)\lambda(\nu) + \sigma_a - \sigma_A}\end{aligned} \tag{31}$$

whenever the invading strain is very similar to the only resident strain.

Now, recall that if a neutral mutant attempts to invade the host, $\mu = \nu$ and, in turn, $f(\mu) = f(\nu)$. When this condition holds, the definition of $E_{1,0}$ simplifies to

$$E_{1,0} = \frac{f(\nu) + f(\nu) - |f(\nu) - f(\nu)|}{2f(\nu)} = \frac{2f(\nu)}{2f(\nu)} = 1.$$

As $E_{0,1} = E_{1,0} = 1$ when $\mu = \nu$, we see that

$$\phi(\nu,\nu) = 1 - \left(1 - \frac{\nu\lambda(\nu)}{(1-k)\lambda(\nu) + \sigma_a - \sigma_A}\right) \cdot 1 - \frac{\nu\lambda(\nu)}{(1-k)\lambda(\nu) + \sigma_a - \sigma_A} \cdot 1 = 0,$$

which, as explained in section 3.2, is precisely what we expect when the mutant is neutral.

Now that we have explicitly defined our mechanistic ϕ, we can plug it into the invasion fitness r from (15). This equation will be central to the adaptive dynamics analysis we perform in the following section.

4 Evolutionary branching

The outcome of evolution under the mechanistic superinfection function is less straightforward (and more interesting!) than in the jump case. Together with the ϕ derived in the previous section, the right choice of α, β and λ produces evolutionary branching in our model.

We henceforth take $\lambda(\mu) = \dfrac{Q}{R + ln(1/\mu)}$, a growth function that decreases to 0 as $\mu \to 0$ and that approaches Q/R as $\mu \to 1$. An example appears in figure 3 below. As described in section 3.1, α and β are functions of the equilibrium pathogen density within the host – that is, $\alpha(\mu) = \tilde{\alpha}(\hat{x}(\mu))$ and $\beta(\mu) = \tilde{\beta}(\hat{x}(\mu))$. We now erase the tildes in these equations and hereafter explicitly consider α and β as functions of $\hat{x}$. Furthermore, we borrow the concept for a simple α from Gilchrist & Coombs (2006), defining $\alpha(\hat{x}(\mu)) = h\hat{x}(\mu)$ for some constant h.

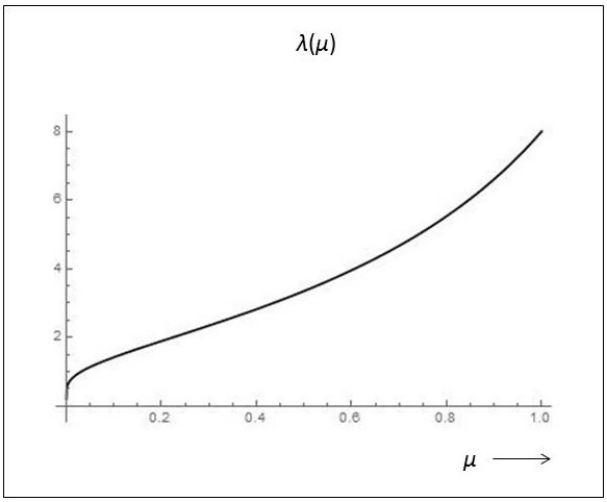

Figure 3. $\lambda(\mu)$ plotted with $Q = 4$ and $R = 0.5$.

In the following subsection, we construct β through critical function analysis, a method that enables us to obtain evolutionary branching at chosen points in our strategy space.

4.1 Finding β: Critical function analysis

Recall from section 1.2 the three conditions a strategy μ^* must satisfy in order to be an evolutionary branching point:

1. μ^* is singular: $\left.\frac{\partial r_\mu(\nu)}{\partial \nu}\right|_{\nu=\mu=\mu^*} = 0.$
2. μ^* is convergence stable: $\left.\frac{\partial^2 r_\mu(\nu)}{\partial \mu \partial \nu}\right|_{\nu=\mu=\mu^*} + \left.\frac{\partial^2 r_\mu(\nu)}{\partial \nu^2}\right|_{\nu=\mu=\mu^*} < 0.$
3. μ^* is not an ESS: $\left.\frac{\partial^2 r_\mu(\nu)}{\partial \nu^2}\right|_{\nu=\mu=\mu^*} > 0.$

Given the ϕ, λ and α we have chosen, what qualities must β have to ensure branching at an arbitrary μ^*? We can convert the above requirements on μ^* into requirements on β with the help of critical function analysis. A nice explanation of the theory behind this technique – plus a substantive example in an SI setting like ours – can be found in [5]. Here we present an outline of the procedure followed by the results it yields in our model.

The first step is to calculate $\left.\frac{\partial r_\mu(\nu)}{\partial \nu}\right|_{\nu=\mu=\mu^*}$, set it equal to 0, and solve for $\beta'(\hat{x}(\mu^*)) := \beta'_{sing}$. This is known as the *singularity condition*, as it pinpoints the slope that β must have at $\hat{x}(\mu^*)$ in order for μ^* to be singular. Next, we calculate $\left.\frac{\partial^2 r_\mu(\nu)}{\partial \mu \partial \nu}\right|_{\nu=\mu=\mu^*}$ (hereafter C_{12}) and $\left.\frac{\partial^2 r_\mu(\nu)}{\partial \nu^2}\right|_{\nu=\mu=\mu^*}$ (hereafter C_{22}). C_{22} depends on both $\beta'(\hat{x}(\mu^*))$ and $\beta''(\hat{x}(\mu^*))$, while C_{12} depends only on $\beta'(\hat{x}(\mu^*))$. Since $\beta'(\hat{x}(\mu^*))$ (and thus C_{12}) is fixed by the singularity condition, we algebraically determine what (if any) $\beta''(\hat{x}(\mu^*))$ assigns C_{22} a value that makes μ^* convergence stable but not evolutionarily stable. If such a $\beta''(\hat{x}(\mu^*))$ exists, we can construct a β that induces branching at μ^*.

In our model, the singularity condition is

$$\beta'_{sing} = \frac{\alpha'(\hat{x}(\mu^*))\hat{x}'(\mu^*) - \hat{I}(\mu^*)\beta(\hat{x}(\mu^*))\partial_\nu[\phi(\mu,\nu) - \phi(\nu,\mu)]_{\mu=\nu=\mu^*}}{\hat{S}(\mu^*)\hat{x}'(\mu^*)}. \quad (32)$$

Note that our simplified mechanistic ϕ (equation (31)) is not differentiable at $\mu = \nu$ due to the absolute value in its numerator. However, the difference

$$M := \phi(\mu,\nu) - \phi(\nu,\mu)$$

is once differentiable there. In fact,

$$\partial_\nu M|_{\mu=\nu=\mu^*} = \frac{f'(\mu^*)}{f(\mu^*)}\Big[1 - \frac{\mu^*\lambda(\mu^*)}{(1-k)\lambda(\mu^*) + \sigma_a - \sigma_A}\Big].$$

As such, the lack of smoothness does not affect our calculation of β'_{sing}. However, M is not differentiable a second time at $\mu = \nu$, and this has important implications for C_{12} and C_{22}. To investigate why this occurs, we first express $\phi(\mu, \nu)$ as

$$\phi(\mu, \nu) = 1 - [(1 - F(\nu)) \cdot E_{1,0} + F(\nu) \cdot E_{0,1}],$$

where F is as described in (28). Recalling that $E_{1,0}$ and $E_{0,1}$ have different values when $f(\nu) < f(\mu)$ and when $f(\nu) > f(\mu)$, we calculate $\partial_{\mu\nu}M$ and $\partial_{\nu\nu}M$ for each case. We find that these derivatives (and in turn C_{12} and C_{22}) are also different for $f(\nu) < f(\mu)$ and $f(\nu) > f(\mu)$. This dichotomy causes C_{12} and C_{22} to be different to the left and right of $\mu = \nu$.

Bearing this in mind, we present the general form of C_{12},

$$\begin{aligned} C_{12} =& \hat{S}'(\mu^*)\beta'_{sing}\hat{x}'(\mu^*) + \hat{I}'(\mu^*)\beta(\hat{x}(\mu^*))\partial_\nu M|_{\mu=\nu=\mu^*} \\ &+ \hat{I}(\mu^*)\beta(\hat{x}(\mu^*))\partial_{\mu\nu}M|_{\mu=\nu=\mu^*}, \end{aligned}$$

and that of C_{22},

$$\begin{aligned} C_{22} =& \hat{S}(\mu^*)[\beta'_{sing}\hat{x}''(\mu^*) + \beta''(\hat{x}(\mu^*))[\hat{x}'(\mu^*)]^2] \\ &- [\alpha'(\hat{x}(\mu^*))\hat{x}''(\mu^*) + \alpha''(\hat{x}(\mu^*))[\hat{x}'(\mu^*)]^2] \\ &+ \hat{I}(\mu^*)\beta(\hat{x}(\mu^*))\partial_{\nu\nu}M|_{\mu=\nu=\mu^*} \\ &+ 2\hat{I}(\mu^*)\beta'_{sing}\hat{x}'(\mu^*)\partial_\nu\phi(\mu,\nu)|_{\mu=\nu=\mu^*}. \end{aligned}$$

We must be careful to respect aforementioned cases when generating numerical examples in the following subsection.

4.2 Examples

In Wolfram Mathematica, we compute C_{12} and C_{22} when $f(\nu) < f(\mu)$ (hereafter ${C_{12}}^{(1)}$ and ${C_{22}}^{(1)}$) and when $f(\nu) > f(\mu)$ (hereafter ${C_{12}}^{(2)}$ and ${C_{22}}^{(2)}$). In portions of the strategy space where f is increasing, ${C_{12}}^{(1)}$ and ${C_{22}}^{(1)}$ are the left derivatives at $\mu = \nu$, while ${C_{12}}^{(2)}$ and ${C_{22}}^{(2)}$ are the right derivatives. The opposite is true when f is decreasing.

We hunt for branching using example singularities from both sides of the maximum of f. First, we select these example singularities μ^* and initial values $\beta(\mu^*)$, plug them into the appropriate C_{12} and C_{22}, and observe the signs of these quantities. Since the third branching condition prescribes that C_{22} must be positive, it follows that C_{12} must be negative enough to ensure $C_{12}+C_{22} < 0$, the second branching condition. Whenever we find a C_{12} equal to some $v < 0$ at a chosen μ^*, we can numerically solve for $\beta''(\hat{x}(\mu^*))$ such that $C_{22} = w$ where $0 < w < |v|$. Then, we can construct a transmission function β that has the slope and concavity required for branching at μ^*.

Initially, we generate a simple β as a Taylor expansion about μ^* with $\beta'(\hat{x}(\mu^*)) = \beta'_{sing}$ and $\beta''(\hat{x}(\mu^*))$ found through the numerical procedure described above. Later, we construct a logistic β that obeys the same rules.

4.2.1 Expansion β

Here we define

$$\begin{aligned}\beta(\hat{x}(\mu)) =&\beta(\hat{x}(\mu^*)) + \beta'(\hat{x}(\mu^*))(\hat{x}(\mu) - \hat{x}(\mu^*)) \\ &+ \beta''(\hat{x}(\mu^*))(\hat{x}(\mu) - \hat{x}(\mu^*))^2 \\ =&\beta(\hat{x}(\mu^*)) + \beta'_{sing}(\hat{x}(\mu) - \hat{x}(\mu^*)) + \beta''(\hat{x}(\mu^*))(\hat{x}(\mu) - \hat{x}(\mu^*))^2.\end{aligned}$$

For two potential branching points, $\mu^* = 0.25$ and $\mu^* = 0.75$, we choose $\beta(\hat{x}(\mu^*))$ and calculate $\beta'(\hat{x}(\mu^*))$ using the formula for β'_{sing} in equation (32). Then, using an example parameter set (see caption of figure 4), we compute ${C_{12}}^{(1)}$ at $\mu^* = 0.25$ and find that it is negative. As described above, we set ${C_{22}}^{(1)}$ equal to a value that satisfies the second and third branching conditions, and we solve this equation to obtain $\beta''(\hat{x}(0.25))$. Because f is increasing at $\mu^* = 0.25$ and because we have used the left derivatives ${C_{12}}^{(1)}$ and ${C_{22}}^{(1)}$ to meet the branching criteria, this singularity will now be a branching point to the left (i.e. for $\nu < \mu^*$).

We similarly choose $\beta(\hat{x}(0.75))$, compute $\beta'(\hat{x}(0.75))$, and solve for $\beta''(\hat{x}(0.75))$ to make $\mu^* = 0.75$ a branching point for $\nu < \mu^*$. However, as f is decreasing at that point, we employ ${C_{12}}^{(2)}$ and ${C_{22}}^{(2)}$ for this procedure.

With β now explicit, we can generate pairwise invasibility plots (figure 4) – and more importantly, mutual invasibility plots (figure 5) – to see where the resident and mutant strains can coexist on the ecological timescale. Recall that in the gray areas of a PIP, the mutant's invasion fitness is positive – that is, the mutant strain can increase in number in the environment set by the resident. On a MIP, the gray areas indicate where both the mutant's invasion fitness against the resident and the resident's invasion fitness against the mutant are positive – that is, where the mutant and resident can invade each other and thus coexist. The invasion fitness, as defined in (15), is $r_\mu(\nu) = \beta(\hat{x}(\nu))\hat{S}(\mu) - [\alpha(\hat{x}(\nu)) + \delta] + \hat{I}(\mu)\Phi(\mu, \nu)$.

From figure 4, we can see that, as expected, both $\mu^* = 0.25$ and $\mu^* = 0.75$ are invasible from below (i.e. when $\nu < \mu^*$). However, they are not invasible by any $\nu > \mu^*$, meaning that they are ESSs from above.

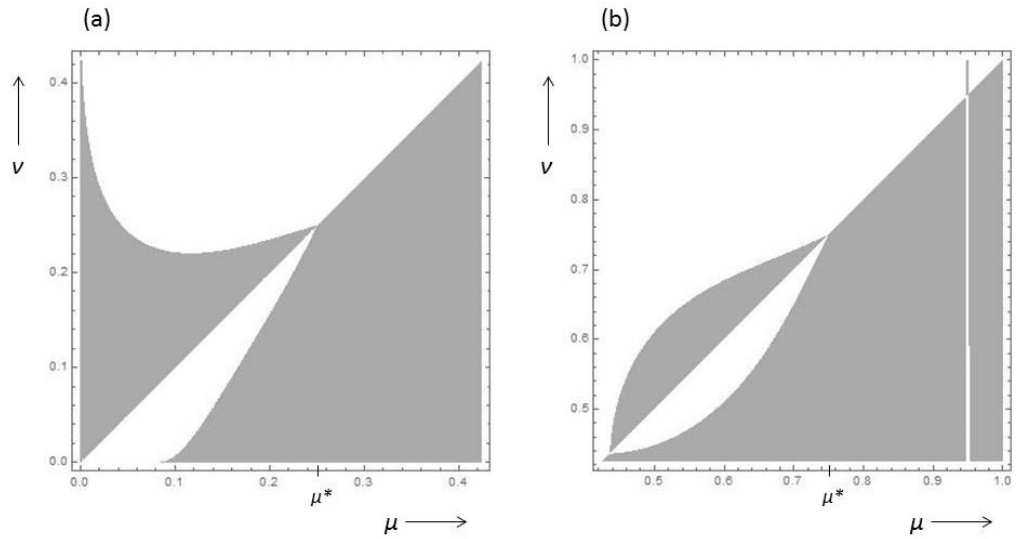

Figure 4. Pairwise invasibility plots with expansion β generated to allow branching around **(a)** $\mu^* = 0.25$ and **(b)** $\mu^* = 0.75$. Parameters used are $b = 1$, $\delta = 0.1$, $Q = 4$, $R = 0.5$, $k = 0.2$, $\sigma_A = 0.05$, $\sigma_a = 0.09$, $c = 0.05$ and $h = 0.05$. In **(a)**, we take $\beta(\hat{x}(0.25)) = 2$. In **(b)**, $\beta(\hat{x}(0.75)) = 5$. In both cases, μ^* is invasible from below but is an ESS from above.

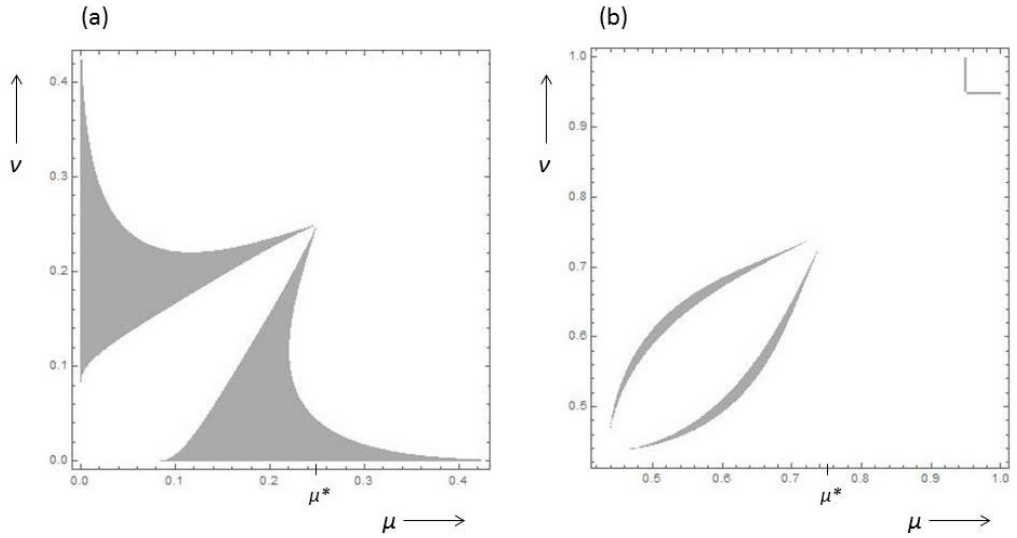

Figure 5. Mutual invasibility plots for the two expansion β functions used in the previous figure. Parameters are unchanged.

Given that our singularities are ESSs to one side but branching points to the other, what will happen to population dimorphisms that arise near them? Will evolutionary branching see to it that two resident traits persist concurrently, or will any coexistence in the vicinity of the monomorphic singularity be merely transient? Boldin & Diekmann (2014) have shown that in the case of such one-sided ESSs, the curvature of the dimorphic resident population's isoclines in the neighborhood of the monomorphic singularity can answer these questions. Therefore, for each of our examples, we plot the dimorphic population's isoclines and investigate its dynamics near μ^*. Specifically, we use phase plane analysis to investigate whether the dimorphic dynamics tend toward or away from μ^*.

The behavior of the dimorphic resident population is described by

$$\begin{cases} \dot{S} = b - \beta(\hat{x}(\mu))SI_\mu - \beta(\hat{x}(\nu))SI_\nu - \delta S \\ \dot{I}_\mu = \beta(\hat{x}(\mu))SI_\mu - [\alpha(\hat{x}(\mu)) + \delta]I_\mu + \Phi(\nu,\mu)I_\mu I_\nu \\ \dot{I}_\nu = \beta(\hat{x}(\nu))SI_\nu - [\alpha(\hat{x}(\nu)) + \delta]I_\nu + \Phi(\mu,\nu)I_\mu I_\nu. \end{cases}$$

From the equation for $\dot{S}$, we readily see that at equilibrium,

$$\hat{S}(\mu,\nu) = \frac{b}{\beta(\hat{x}(\mu))\hat{I}_\mu(\mu,\nu) + \beta(\hat{x}(\nu))\hat{I}_\nu(\mu,\nu) + \delta}.$$

When a mutant m is introduced, the population dynamics become

$$\begin{cases} \dot{S} = b - \beta(\hat{x}(\mu))SI_\mu - \beta(\hat{x}(\nu))SI_\nu - \beta(\hat{x}(m))SI_m - \delta S \\ \dot{I}_\mu = \beta(\hat{x}(\mu))SI_\mu - [\alpha(\hat{x}(\mu)) + \delta]I_\mu + \Phi(\nu,\mu)I_\mu I_\nu + \Phi(m,\mu)I_\mu I_m \\ \dot{I}_\nu = \beta(\hat{x}(\nu))SI_\nu - [\alpha(\hat{x}(\nu)) + \delta]I_\nu + \Phi(\mu,\nu)I_\mu I_\nu + \Phi(m,\nu)I_\nu I_m \\ \dot{I}_m = \beta(\hat{x}(m))SI_m - [\alpha(\hat{x}(m)) + \delta]I_m + \Phi(\mu,m)I_m I_\mu + \Phi(\nu,m)I_m I_\nu. \end{cases}$$

The invasion fitness of the mutant is

$$r_{\mu,\nu}(m) = \beta(\hat{x}(m))\hat{S}(\mu,\nu) - [\alpha(\hat{x}(m)) + \delta] + \Phi(\mu,m)I_\mu + \Phi(\nu,m)I_\nu.$$

By the selective neutrality of the residents, it holds that $r_{\mu,\nu}(\mu) = r_{\mu,\nu}(\nu) = 0$. As such,

$$\begin{aligned} &\beta(\hat{x}(\mu))\hat{S}(\mu,\nu) - [\alpha(\hat{x}(\mu)) + \delta] + \Phi(\mu,\mu)\hat{I}_\mu(\mu,\nu) + \Phi(\nu,\mu)\hat{I}_\nu(\mu,\nu) = 0 \\ &\iff \Phi(\nu,\mu)\hat{I}_\nu(\mu,\nu) = \alpha(\hat{x}(\mu)) + \delta - \beta(\hat{x}(\mu))\hat{S}(\mu,\nu) \\ &\iff \hat{I}_\nu(\mu,\nu) = \frac{\beta(\hat{x}(\mu))}{\Phi(\nu,\mu)}[\hat{S}(\mu) - \hat{S}(\mu,\nu)] \\ &\iff \hat{I}_\nu(\mu,\nu) = \frac{\beta(\hat{x}(\mu))}{\Phi(\mu,\nu)}[\hat{S}(\mu,\nu) - \hat{S}(\mu)]. \end{aligned}$$

Similarly,

$$\begin{aligned} &\beta(\hat{x}(\nu))\hat{S}(\mu,\nu) - [\alpha(\hat{x}(\nu)) + \delta] + \Phi(\mu,\nu)\hat{I}_\mu(\mu,\nu) + \Phi(\nu,\nu)\hat{I}_\nu(\mu,\nu) = 0 \\ &\iff \hat{I}_\mu(\mu,\nu) = \frac{\beta(\hat{x}(\nu))}{\Phi(\mu,\nu)}[\hat{S}(\nu) - \hat{S}(\mu,\nu)]. \end{aligned}$$

The interior equilibrium of this system is thus

$$\hat{S}(\mu,\nu) = \frac{b}{\beta(\hat{x}(\mu))\hat{I}_\mu(\mu,\nu) + \beta(\hat{x}(\nu))\hat{I}_\nu(\mu,\nu) + \delta}$$
$$\hat{I}_\mu(\mu,\nu) = \frac{\beta(\hat{x}(\nu))}{\Phi(\mu,\nu)}[\hat{S}(\nu) - \hat{S}(\mu,\nu)]$$
$$\hat{I}_\nu(\mu,\nu) = \frac{\beta(\hat{x}(\mu))}{\Phi(\mu,\nu)}[\hat{S}(\mu,\nu) - \hat{S}(\mu)].$$

Note that because our monomorphic between-host dynamics match those in [3], so too do our dimorphic dynamics and equilibria. Note also that because we are now dealing with a dimorphic resident population, the assumption of small mutation steps is no longer sufficient to allow us to use the simplified mechanistic superinfection function given in (31). Instead, we use the full form of ϕ from (29) to compute Φ from (13).

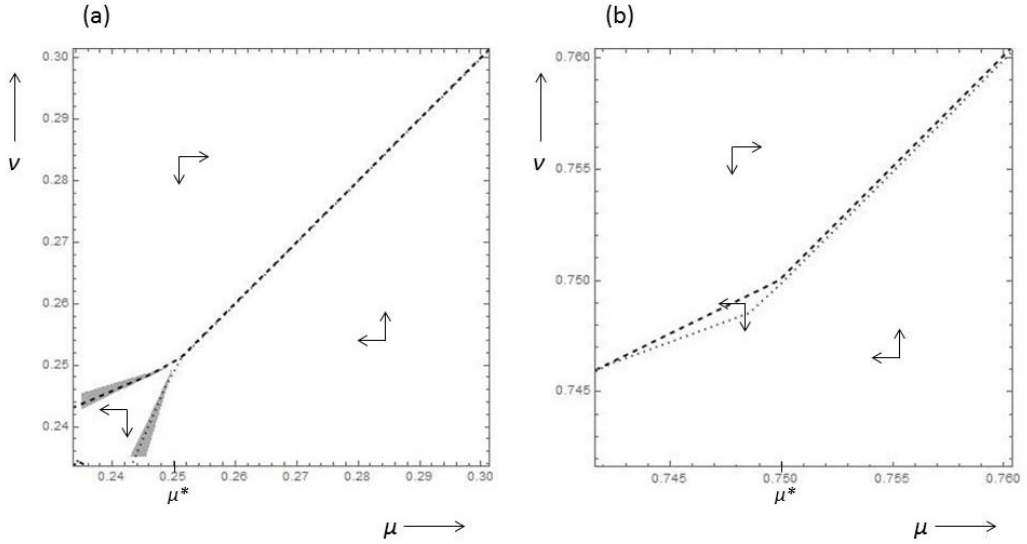

Figure 6. Phase plane analysis of the dimorphic resident dynamics near **(a)** $\mu^* = 0.25$ and **(b)** $\mu^* = 0.75$, using the expansion β generated for each case. In both cases, the dimorphic population tends away from the monomorphic singularity, thus indicating evolutionary branching. The dashed isocline corresponds to $\frac{\partial r_{\mu,\nu}(m)}{\partial m}\Big|_{m=\mu} = 0$, while the dotted one corresponds to $\frac{\partial r_{\mu,\nu}(m)}{\partial m}\Big|_{m=\nu} = 0$.

The isoclines we plot near each monomorphic singularity are the two curves $\frac{\partial r_{\mu,\nu}(m)}{\partial m}\Big|_{m=\mu} = 0$ and $\frac{\partial r_{\mu,\nu}(m)}{\partial m}\Big|_{m=\nu} = 0$. Phase plane analysis (fig-

ure 6) confirms that both $\mu^* = 0.25$ and $\mu^* = 0.75$ do indeed function as evolutionary branching points.

It is now of interest to determine what will happen to the populations rendered dimorphic by the branching event. We address this question in the case of $\mu^* = 0.25$ by examining its dimorphic singularity. Zooming out on figure 6a affords us a rough visual approximation of that singularity, which is found at the two points of intersection of the dimorphic isoclines inside the coexistence region (figure 7a). Although these intersection points are difficult to see from the graphic, we recover their coordinates using Mathematica's `FindRoot` function. They are $(0.089, 0.176)$ and $(0.176, 0.089)$ under the parameter set we have chosen. Note that these coordinates are symmetrical and that $\mu = 0.089$ and $\nu = 0.176$ are the two resident trait values.

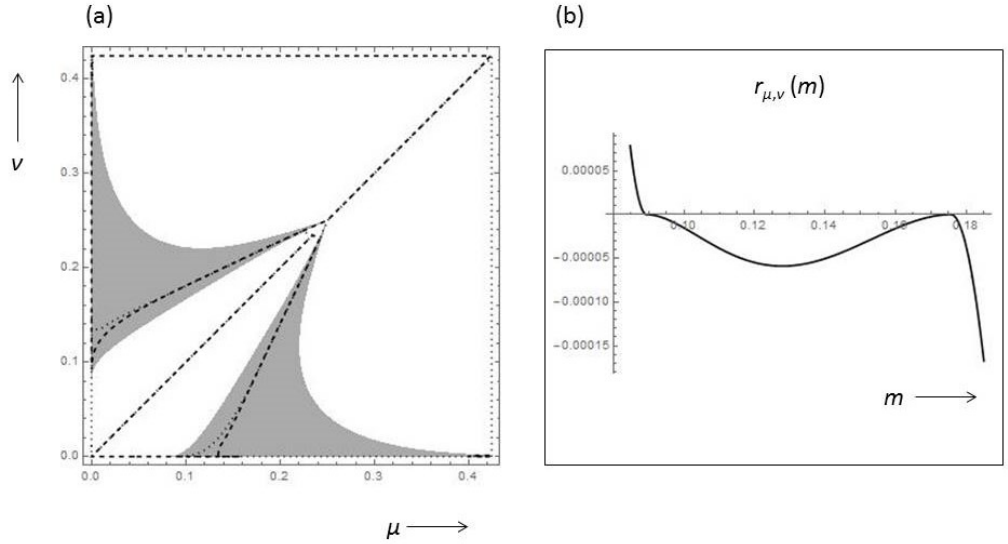

Figure 7. **(a)** MIP near the branching point $\mu^* = 0.25$ overlaid with the dimorphic population's isoclines. In the shaded region, the isoclines intersect at $(0.089, 0.176)$ and at $(0.176, 0.089)$, which are the coordinates of the dimorphic singularity. All parameters are as in figure 4, and the dotted and dashed isoclines are as in figure 6. **(b)** Plot of the dimorphic invasion fitness at the dimorphic singularity seen in (a). As $r_{\mu,\nu}(m)$ is positive to the left of the lower resident trait but negative to its right, that trait is invasible from the left but is an ESS to the right. The higher resident trait value is strictly an ESS, as it is a local fitness maximum and is thus not invasible by any nearby trait.

From the plot of the invasion fitness at the dimorphic singularity (image 7b), it is apparent that the left resident trait is invasible to the left but is an

ESS to the right, just like the monomorphic singularity. The right resident trait is an ESS.

4.2.2 Logistic β

We now introduce a more biologically realistic transmission function,

$$\beta(\hat{x}(\mu)) = \frac{K\beta_0 e^{q\hat{x}(\mu)}}{K + \beta_0(e^{q\hat{x}(\mu)} - 1)} + L.$$

Under this β, the transmission rate increases logistically with the pathogen load before eventually plateauing at $K + L$. Here, q is analogous to the intrinsic growth rate in a function modeling population size over time; that is, it represents the proportional change in β per unit change in the within-host equilibrium pathogen density. β_0 serves as an initial value parameter such that $\beta(0) = \beta_0 + L$. Note that this means that if β were to obey the above logistic definition globally, the transmission rate would be nonzero even at $\hat{x}(\mu) = 0$. However, β need only locally take this form, meaning that it can behave differently and become zero near the origin.

We choose an example parameter set and generate the PIP and MIP in figure 8, finding a singularity at $\mu^* = 0.33$. Similarly to the monomorphic singularities we examined under the expansion β, the μ^* we have here is invasible from below but is an ESS from above.

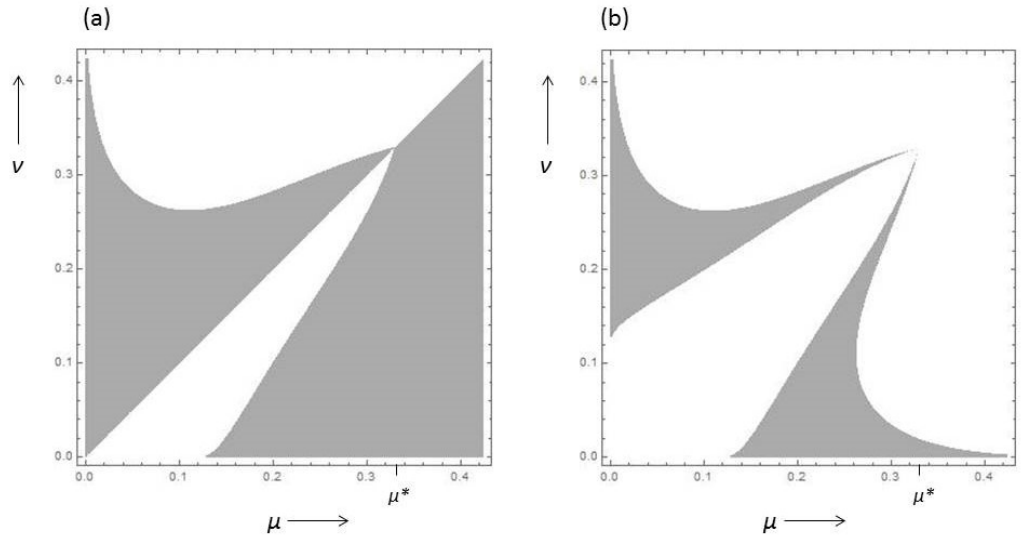

Figure 8. **(a)** PIP and **(b)** MIP under the logistic β function with $K = 255.039$, $\beta_0 = 0.101$, $q = 0.057$ and $L = 1.38$. Both plots closely resemble those that result from the expansion β generated about $\mu^* = 0.25$, though here the singularity occurs at $\mu^* = 0.33$.

We again plot the dimorphic resident population's isoclines over the MIP and perform phase plane analysis to determine whether or not the areas of coexistence harbor evolutionary branching in the long term (figure 9). As in the expansion β case, the dimorphic dynamics tend away from the monomorphic singularity, meaning that the two resident traits will remain divergent from one another on the evolutionary timescale. To understand what will ultimately happen to each one, we plot $r_{\mu,\nu}(m)$ against m at the dimorphic singularity (where $\mu = 0.100$ and $\nu = 0.215$). We see once more that the higher dimorphic resident is strictly an ESS, while the lower resident is invasible from the left but is an ESS to the right (figure 10).

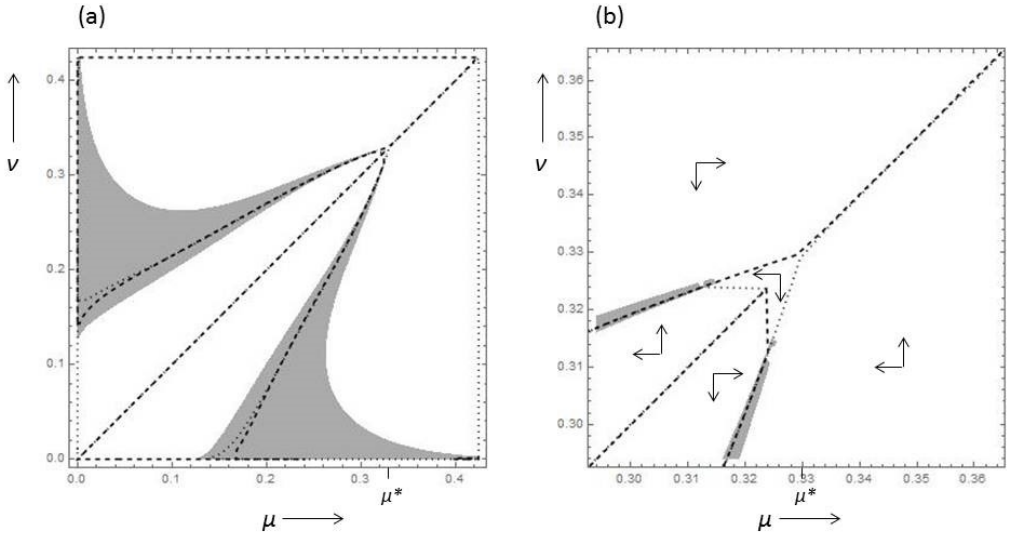

Figure 9. **(a)** Overlay of the logistic β's dimorphic resident isoclines with the monomorphic population's MIP. As before, the dashed line represents the μ-isocline, while the dotted one represents the ν-isocline. The two intersections of these isoclines in the shaded area indicate the dimorphic singularity, whose coordinates are $(0.100, 0.215)$ and $(0.215, 0.100)$. **(b)** Phase plane analysis in the neighborhood of the monomorphic singularity $\mu^* = 0.33$. As under the expansion β, the dimorphic dynamics tend away from the monomorphic singularity, thus indicating that this singularity ultimately acts as a branching point.

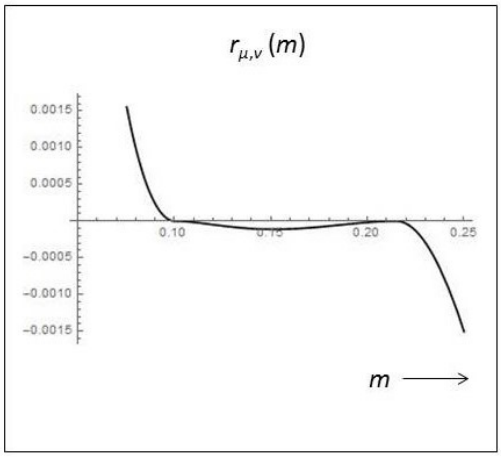

Figure 10. Plot of $r_{\mu,\nu}(m)$ at the dimorphic singularity. As in the $\mu^* = 0.25$ case of the expansion β, the higher resident is an ESS, while the lower one is invasible from the left but is an ESS to the right.

5 Discussion

In this thesis, we have addressed the question of whether and how multiple pathogen strains with different mutation probabilities can persist and coexist in their host population on the evolutionary timescale. Motivated by the work of O'Fallon (2011) and Regoes et al. (2013), we modeled the within- and between-host dynamics of a pathogen under the biological assumption of a trade-off between replication speed and fidelity. Then, we used the framework of adaptive dynamics to show that in the presence of superinfection and under both a caricatural and a biologically realistic transmission function, evolutionary branching of strains with distinct mutation probabilities is possible.

We based our modeling techniques on those of Boldin & Diekmann (2008), who used them to study the evolution of a pathogen's within-host replication rate. The evolutionary branching we have uncovered occurs at singularities that are branching points to one side but ESSs to the other: so-called one-sided ESSs. Boldin & Diekmann (2014) showed that this phenomenon can be explained by the non-smoothness of the superinfection function.

Our results differ from those of O'Fallon in two key ways: First, unlike him (but like Regoes et al.) we employ analytical methods in lieu of a simulation approach to show the persistence of multiple mutation probabilities over time. Second, our divergent strains are not vastly different from one another: The distance between two resident strategies in the early stages of branching is modest compared to that between the very low and very high optima uncovered by O'Fallon.

Starting from a more intricate within-host model than ours, Regoes et al. also find that two ideal mutation rates, identified as the intersection points of a speed-fidelity trade-off function and a fitness ridge, need not necessarily be far apart. However, because theirs is an optimization model, those two traits cannot coexist in the population.

Some other analytical studies on pathogen mutation rates, such as [1] and [2], approach this topic from perspectives entirely different from ours. Belavkin et al. (2016) conceptualize fitness geometrically, defining it as the distance between a given trait value and that of a theoretically optimal organism. Whereas we adopt the core assumptions of adaptive dynamics, including that of small mutation steps, their model deliberately allows for mutations

of any size. As their examples grow more involved, they utilize simulation to uncover mutation rates that evolve to a minimum distance from an ideal over the course of many generations.

Birch & Bolker (2015) create a compartmental epidemiological model with seasonal forcing to study the evolution of virulence in a pathogen, and they incorporate mutation rate in a diffusion term as part of the density dynamics of the infected population. Unlike us, they do not allow for any within-host competition. Although the adaptive trait of their focus is virulence, their model nevertheless yields an important implication for the mutation rate, namely that the only ESS value for it is zero under the assumptions and modeling choices they made.

Our work serves as an entry point to the study of pathogen mutation probabilities via the theory of adaptive dynamics, and it can potentially be extended in several ways. First, one could investigate what happens to each of our evolutionary branches in the future: Will further branching occur? Will the branch established by one of the dimorphic residents ultimately die out? Making other choices for β and/or performing critical function analysis on α could reveal yet more ways for branching to occur – or could highlight situations in which branching is impossible. Choosing or deriving a different kind of superinfection function could also affect the evolutionary properties of our model. So, too, could more elaborate treatment of the within-host dynamics, like that found in [3] and [15].

References

[1] R.V. Belavkin, A. Channon, E. Aston, J. Aston, R. Krašovec, and C.G. Knight. Monotonicity of fitness landscapes and mutation rate control. *Journal of Mathematical Biology*, 73:1491–1524, 2016.

[2] M. Birch and B.M. Bolker. Evolutionary stability of minimal mutation rates in an evo-epidemiological model. *Bulletin of Mathematical Biology*, 77:1985–2003, 2015.

[3] B. Boldin and O. Diekmann. Superinfections can induce evolutionarily stable coexistence of pathogens. *Journal of Mathematical Biology*, 56:635–672, 2008.

[4] B. Boldin and O. Diekmann. An extension of the classification of evolutionarily singular strategies in adaptive dynamics. *Journal of Mathematical Biology*, 69:905–940, 2014.

[5] B. Boldin, S.A.H. Geritz, and É. Kisdi. Superinfections and adaptive dynamics of pathogen virulence revisited: a critical function analysis. *Evolutionary Ecology Research*, 11:153–175, 2009.

[6] M.J. Dapp, R.H. Heineman, and L.M. Mansky. Interrelationship between HIV-1 fitness and mutation rate. *Journal of Molecular Biology*, 425:41–53, 2013.

[7] U. Fahnøe, A.G. Pedersen, C. Dräger, R.J. Orton, S. Blome, D. Höper, M. Beer, and T.B. Rasmussen. Creation of functional viruses from non-functional cDNA clones obtained from an RNA virus population by the use of ancestral reconstruction. *PLoS ONE*, 10:1–17, 10 2015.

[8] V. Furió, A. Moya, and R. Sanjuán. The cost of replication fidelity in an RNA virus. *Proceedings of the National Academy of Sciences of the United States of America*, 102:10233–10237, 2005.

[9] V. Furió, A. Moya, and R. Sanjuán. The cost of replication fidelity in human immunodeficiency virus type 1. *Proceedings of the Royal Society B*, 274:225–230, 2007.

[10] S.A.H. Geritz, É. Kisdi, G. Meszéna, and J.A.J. Metz. Evolutionarily singular strategies and the adaptive growth and branching of the evolutionary tree. *Evolutionary Ecology*, 12:35–57, 1998.

[11] M.A. Gilchrist and D. Coombs. Evolution of virulence: Interdependence, constraints, and selection using nested models. *Theoretical Population Biology*, 69:145–153, 2006.

[12] A.J. Herr, L.N. Williams, and B.D. Preston. Antimutator variants of DNA polymerases. *Critical Reviews in Biochemistry and Molecular Biology*, 46:548–570, 2011.

[13] P. Jagers. *Branching Processes with Biological Applications*. John Wiley & Sons, 1975.

[14] B. O'Fallon. Two optimal mutation rates in obligate pathogens subject to deleterious mutation. *Journal of Theoretical Biology*, 276:150–158, 2011.

[15] R. R. Regoes, S. Hamblin, and M. M. Tanaka. Viral mutation rates: modelling the roles of within-host viral dynamics and the trade-off between replication fidelity and speed. *Proceedings of the Royal Society B*, 280:1–9, 2013.

[16] E.C. Smith and M.R. Denison. Coronaviruses as DNA wannabes: a new model for the regulation of RNA virus replication fidelity. *PLoS Pathogens*, 9:1–4, 12 2013.

[17] H.R. Thieme. Pathogen competition and coexistence and the evolution of virulence. In Y. Takeuchi, Y. Iwasa, and K. Sato, editors, *Mathematics for Life Science and Medicine*, pages 123–153. Springer, 2007.